

DEVELOPMENT OF A MULTISCALE MODEL OF THE
LUMBAR SPINE: APPLICATION FOR PERSONS
WITH A LOWER-LIMB AMPUTATION

by

Jasmin D. Honegger

© Copyright by Jasmin D. Honegger, 2017

All Rights Reserved

A thesis submitted to the Faculty and the Board of Trustees of the Colorado School of Mines in partial fulfillment of the requirements for the degree of Master of Science (Mechanical Engineering).

Golden, Colorado

Date _____

Signed: _____
Jasmin D. Honegger

Signed: _____
Dr. Anthony J. Petrella
Thesis Advisor

Golden, Colorado

Date _____

Signed: _____
Dr. Gregory Jackson
Professor and Head
Department of Mechanical Engineering

ABSTRACT

Low back pain (LBP) is a large problem in the general population and especially among people with a lower-limb amputation (LLA). The primary causes of LBP for people with LLA are whole-body kinematic and muscle asymmetries [1]. However, the sources of LBP are known to exist at the tissue-level such as within the intervertebral discs or facet joint capsules [2]. No previous study has identified the connection between determining the source of pain at the tissue-level and the cause of pain at the whole-body level. Identification of this interconnectivity is required for better understanding of LBP and therapeutic intervention for people with LLA. The purpose of this research was to create a multiscale model of the human lumbar spine in order to help identify and characterize the interconnectivity between whole-body biomechanics and tissue-level metrics leading to LBP for LLA. The results revealed that people with LLA have greater tissue-level loads than able-bodied individuals and suggest that people with LLA may perform certain motions with a more consistent strategy as compared to people without an amputation. These findings help to improve the current understanding of multiscale lumbar spine biomechanics, elucidate the greater risk for LBP in people with LLA, and can help to inform future treatment for biomechanical LBP.

TABLE OF CONTENTS

ABSTRACT	iii
LIST OF FIGURES	vi
LIST OF TABLES	viii
LIST OF SYMBOLS	ix
LIST OF ABBREVIATIONS	x
CHAPTER 1 INTRODUCTION	1
CHAPTER 2 REVIEW OF LITERATURE	3
2.1 Anatomy of the lumbar spine	3
2.2 Low back pain	6
2.2.1 Lumbar spine kinematics and structural failure	7
2.2.2 Muscle function and conditions	12
2.2.3 Tissue-level conditions	14
2.2.4 Summary	16
2.3 Persons with a lower-limb amputation	17
2.4 Biomechanical modeling techniques	18
2.4.1 Macroscale modeling	18
2.4.2 Mesoscale modeling	21
2.4.3 Multiscale modeling	24
CHAPTER 3 DEVELOPMENT OF A MULTISCALE MODEL OF THE LUMBAR SPINE: APPLICATION FOR PERSONS WITH A TRANSTIBIAL AMPUTATION DURING SIT-TO-STAND	29

3.1	Abstract	29
3.2	Introduction	30
3.3	Methods	32
3.3.1	Multiscale model development	32
3.3.2	Experimental protocol	34
3.3.3	Simulation workflow	34
3.3.4	Output and statistical analysis	35
3.4	Results	37
3.5	Discussion	38
3.6	Conclusions	42
	CHAPTER 4 CONCLUSIONS	45
	REFERENCES CITED	46
	APPENDIX - SUPPORTING TABLES	58

LIST OF FIGURES

Figure 2.1	The lumbar vertebral column (shown and magnified in pink) located below the thoracic vertebrae and above the sacrum	4
Figure 2.2	Features of healthy lumbar vertebrae: vertebral body (VB), pedicle (P), transverse process (TP), vertebral foramen (VF), lamina (L), interior articular facet (IAF), spinous process (SP), pars interarticularis (PI), superior articular process (SAP), superior articular facet (SAF), accessory process (AP), interior articular process (IAP) (adapted from) . . .	5
Figure 2.3	Structure of a lumbar intervertebral disc (adapted from)	5
Figure 2.4	Example of a spondylometer, instrument consisting of two angled rods and a protractor, used to measure spinal mobility	8
Figure 2.5	Lumbar spine compression fracture located at the L4 level	10
Figure 2.6	Lumbar spine bending fracture (blue arrow indicates intact pars interarticularis, red arrow indicates fractured pars interarticularis)	11
Figure 2.7	Schematic of a trigger point complex	13
Figure 2.8	Example of a radial fissure in internal disc disruption (adapted from) . . .	16
Figure 2.9	Musculoskeletal model of the human lumbar spine developed in OpenSim. Muscle wrapping objects are shown in blue mesh and muscle fascicles shown in red	20
Figure 2.10	Finite element model of the human lumbar spine developed in ABAQUS. Bony elements are shown as white elements and intervertebral discs as blue elements	23
Figure 2.11	Diagrams indicating the line of action of the rectus femoris (blue line) and its hip joint reaction force (green/red arrow). The left column shows the discretized hip joint FE model and the right column shows representative positions from the musculoskeletal model	27

Figure 3.1	Workflow of the multiscale model development: (a) Scaling and registration of the FE model geometry to the musculoskeletal model, (b) determination of lumbar spine muscle attachment locations, (c) application of fixed centers-of-rotation in each FE model intervertebral joint, (d) prescription of L5 rotational boundary conditions for match the experimental motion, and (e) application of joint contact forces and moments for the torso-L1 joint and lumbar spine muscle forces to the FE model.	33
Figure 3.2	Scatter plots of each lumbar spine rotational DOF during sit-to-stand versus each tissue-level metric to determine the most appropriate regression model for each comparison for able-bodied (AB) participants and participants with TTA. Facet joint contact force plots labeled as “With +/–” and “Without +/–” to denote force calculation method.	36
Figure 3.3	Multiscale lumbar spine kinematic evaluation (mean \pm 1 standard deviation) for all participants between the OpenSim input (black curves) and Abaqus output (green curves) kinematics.	38
Figure 3.4	Trunk-pelvis kinematics (mean \pm 1 standard deviation) for participants with TTA (blue curves) and able-bodied (AB) participants (red curves) determined by inverse kinematics within the musculoskeletal model framework.	39
Figure 3.5	Regression model results (grey curves) for annulus fibrosis vM stress vs. flexion/extension, facet joint contact force vs. axial rotation, and intradiscal pressure vs. flexion/extension for each participant group (TTA (blue triangles): participants with TTA, AB (red circles): able-bodied participants, ALL: all participants). R^2 values are indicated for each comparison.	44

LIST OF TABLES

Table 2.1	Ranges of lumbar segmental motion in males 25-36 years old. (Based on Percy et al. 1984 and Percy and Tibrewal 1984)	9
Table 3.1	Mean (\pm standard deviation) of peak annulus fibrosis vM stress, peak facet joint contact force, and average intradiscal pressure for participants with TTA and able-bodied participants at each lumbar spine level and averaged across levels ($\alpha = 0.05$; significant difference denoted by *).	40
Table 3.2	Results from the regression analyses for each participant group (ALL: all participants, AB: able-bodied participants, TTA: participants with TTA). $R^2 \geq 0.7$ are shown in bold.	40
Table A.1	The extent to which proposed causes of back pain satisfy the postulates for a structure to be a source of LBP	58

LIST OF SYMBOLS

System mass matrix	$M(q)$
Generalized positions	q
Generalized velocities	\dot{q}
Generalized accelerations	\ddot{q}
Coriolis and centrifugal forces	$C(q, \dot{q})$
Gravitational forces	$G(q)$
Generalized forces	τ

LIST OF ABBREVIATIONS

Low back pain	LBP
Lower-limb amputation	LLA
Transtibial amputation	TTA
Transfemoral amputation	TFA
Musculoskeletal modeling	MSM
Finite element	FE
Magnetic resonance imaging	MRI
Activities of daily living	ADL
Internal disc disruption	IDD
Degrees of freedom	DOF
Vertebral body replacement	VBR
Computed tomography	CT
Intervertebral disc	IVD
Electromyography	EMG
Ground reaction force	GRF
von Mises	vM
Able-bodied	AB

CHAPTER 1

INTRODUCTION

Low back pain (LBP) is a common problem in the general population and has an even greater prevalence among people with a lower-limb amputation (LLA) [3, 4]. For many people with LLA, LBP is known as a secondary condition commonly associated with altered movement strategies resulting from adaptation to limb loss [5]. Low back pain for LLA is primarily caused by whole-body kinematic and muscle asymmetries [1]. The sources of LBP are known to exist at the tissue-level such as within the intervertebral discs or facet joint capsules [2]. However, the current standard of care to treat LLA with LBP is physical therapy, which is an intervention at the whole-body level. Research to bridge the gap between determining the source of pain at the tissue-level and the cause of pain at the whole-body level is required for better understanding of LBP and therapeutic intervention. Computational modeling allows for estimation of biological quantities that are difficult or impossible to measure *in vivo*. Specifically, musculoskeletal models allow for prediction of muscle and joint reaction forces, and finite element models allow for estimation of tissue-level parameters such as stresses and forces within soft tissues. Both modeling frameworks are beneficial for specific research questions. However, musculoskeletal models lack the fidelity to incorporate tissue-level parameters such as detailed joint contact models and constitutive modeling of materials. Additionally, finite element models are too computationally expensive to model the whole body. Multiscale modeling allows for two or more scales to be combined into a single framework with interaction between scale levels. Thus, the purpose of this research was to create a multiscale model of the human lumbar spine in order to help identify and characterize the link between whole-body biomechanics and tissue-level metrics leading to LBP. The model was applied to people with and without LLA. The results of this work will help to improve the current understanding of whole-body and tissue-level lumbar spine

biomechanics and elucidate the greater risk for LBP in people with LLA. The following are the aims and hypotheses of this work:

- **Aim 1:** Develop a multiscale model of the lumbar spine.
 - Objective 1: A whole-body musculoskeletal model with a detailed lumbar spine will be created.
 - Objective 2: A finite element model of the lumbar spine will be adapted to correspond to the musculoskeletal model scale, orientation, and kinematic constraints.

- **Aim 2:** Identify differences in whole-body biomechanics and tissue-level metrics within the lumbar spine between people with TTA and able-bodied individuals during sit-to-stand.
 - Hypothesis 1 (H1): People with TTA will have greater ranges of trunk-pelvis motion than able-bodied participants [6].
 - Hypothesis 2 (H2): People with TTA will have greater peak stress in the annulus fibrosis, greater peak facet joint contact forces, and greater average intradiscal pressure than able-bodied participants.

- **Aim 3:** Investigate the link between whole-body biomechanics and tissue-level metrics within the lumbar spine.
 - Hypothesis 1 (H1): Maximum lumbar spine flexion will correlate with peak annulus fibrosis stress.
 - Hypothesis 2 (H2): Maximum lumbar spine axial rotation will correlate with peak facet joint contact force.
 - Hypothesis 3 (H3): Increased lumbar spine flexion will correlate with greater average intradiscal pressure.

CHAPTER 2

REVIEW OF LITERATURE

The following is a review of scientific literature that provides evidence to motivate the development and analysis of multiscale modeling of the human lumbar spine in order to better understand the etiology and pathogenesis of low back pain for individuals with a lower-limb amputation.

2.1 Anatomy of the lumbar spine

The lowest section of vertebrae in the human spine is the lumbar vertebral column, consisting of five individual bodies (Figure 2.1). The vertebral levels are denoted as L1-L5 with the first level being the most superior and closest to the thoracic vertebrae above. The main function of the lumbar spine is to provide support for weight-bearing and the structures of the lumbar spine protect the spinal cord and nerves.

There are key features with specific functions on typical lumbar vertebrae (Figure 2.2). The vertebral body is the largest block of bone on a vertebra and is the structure that provides the most weight-bearing support. Two projections of bone extending from the vertebral body are the pedicles that each connect to a sheet of bone called the lamina. Together, these structures protect the spinal cord, which runs through the vertebral foramen. Extending from the laminae and pedicles are the various processes of the lumbar spine. The transverse processes are large portions of bone that extend from the pedicles in the transverse direction and serve as areas for muscle attachments. The posterior bony projection from the proximal end of the transverse process is known as the accessory process. Each vertebra has four articular processes: a left and right inferior articular process; and a left and right superior articular process. Smooth areas of bone covered by articular cartilage are located on the medial surface of the superior articular processes and the lateral surface of the inferior articular processes. These areas are known as the facets of each articular process and make up



Figure 2.1: The lumbar vertebral column (shown and magnified in pink) located below the thoracic vertebrae and above the sacrum [7]

the facet (or zygapophysial) joints of the lumbar spine. The parts of each vertebra located between the superior and inferior articular processes is known as the pars interarticularis. A narrow portion of bone that resembles the shape of an axe blade and projected posteriorly from the laminae is the spinous process. This process serves as an attachment site for muscles and ligaments of the lumbar spine. A visual summary of these key features of the lumbar spine is shown in Figure 2.2.

The intervertebral disc is an integral component of lumbar spine anatomy, specifically allowing for flexion, extension, lateral bending, and shock absorption. Each disc is located in between the vertebral endplates of two adjacent vertebral bodies. The two primary components of the intervertebral disc are the nucleus pulposus and annulus fibrosus. The nucleus is the soft inner core of the disc. It is comprised of mucoïd material and collagen fibers that allow the disc to withstand torsional and compressive forces. The annulus fibrosus is the tough outer ring of the intervertebral disc. It consists of sheets of collagen fibers called

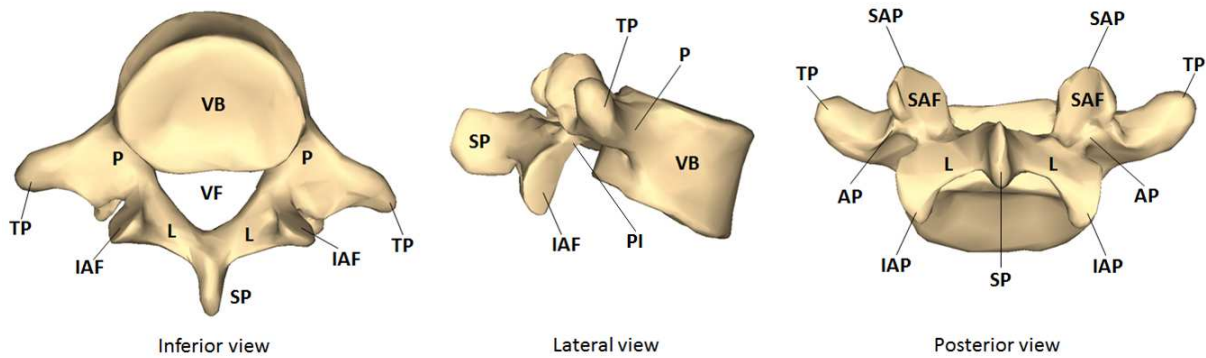


Figure 2.2: Features of healthy lumbar vertebrae: vertebral body (VB), pedicle (P), transverse process (TP), vertebral foramen (VF), lamina (L), interior articular facet (IAF), spinous process (SP), pars interarticularis (PI), superior articular process (SAP), superior articular facet (SAF), accessory process (AP), interior articular process (IAP) (adapted from [8])

lamellae that enclose the nucleus pulposus and provide a secure connection to adjacent vertebrae (Figure 2.3). An important feature of the intervertebral disc is that for any applied load, equilibrium will be achieved due to the tension developed in the annulus fibers exactly balancing the radial pressure exerted by the nucleus [2].

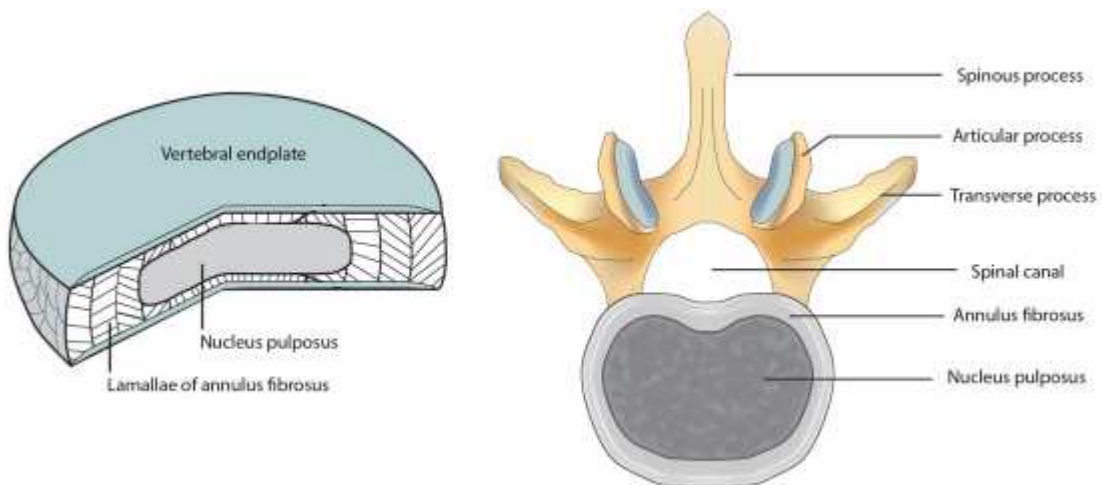


Figure 2.3: Structure of a lumbar intervertebral disc (adapted from [9])

2.2 Low back pain

Approximately 80% of adults experience low back pain (LBP) at some point during the course of their life, qualifying it as a major socioeconomic problem for the general population [10]. The International Association for the Study of Pain (IASP) defines LBP as pain perceived as arising from either the lumbar spine or the sacrum or a combination of both these regions [11]. The majority of LBP is acute, which refers to short term pain that lasts a few days to a few weeks and often resolves on its own, while chronic LBP is characterized as pain that remains for 12 weeks or longer. Chronic LBP is a more serious condition and typically requires treatment or surgery. The causes of LBP originate primarily from mechanical events; however, nearly every structure in the lumbar spine has been suggested as a possible source of back pain at various points in history. In *Clinical and Radiological Anatomy of the Lumbar Spine*, Bogduk defines possible causes for LBP by modifying criteria from Koch's postulates for bacterial diseases as follows [2]:

An anatomical structure may cause LBP if,

1. "the structure should have a nerve supply, for without access to the nervous system it could not evoke pain."
2. "the structure should be capable of causing pain similar to that seen clinically. Ideally, this should be demonstrated in normal volunteers, for inferences drawn from clinical studies may be compromised by observer bias or poor patient reliability."
3. "the structure should be susceptible to diseases or injuries that are known to be painful. Ideally, such disorders should be evident upon investigation of the patient but this may not always be possible. Certain conditions may not be detectable using currently available imaging techniques, whereupon the next line of evidence stems from post-mortem studies or biomechanical studies which can provide at least prima facie evidence of the types of disorders or injuries that might affect the structure."

4. “the structure should have been shown to be a source of pain in patients, using diagnostic techniques of known reliability and validity. From such data, a measure of the prevalence of the condition in question can be obtained to indicate whether the condition is a rarity or oddity, or a common cause of back pain.”

Utilizing these postulates, analysis of the lumbar spine and sacrum anatomy can lead to possible sources of LBP. These sources can be organized into three groups: structural failure due to kinematics, muscle conditions, and tissue-level conditions.

2.2.1 Lumbar spine kinematics and structural failure

Repetitive movements past the normal range of motion of the lumbar spine along with increased loading can result in fatigue failure of various spinal elements, which in turn leads to LBP. The primary movements of the lumbar spine are axial compression/distraction, flexion/extension, axial rotation, and lateral flexion. The range of motion of the lumbar spine has been studied using cadavers, radiographs, and spondylometers (Figure 2.4). Though total ranges of motion do not offer diagnostic insight, they present quantified information on spinal function that demonstrate the underlying biochemical and biomechanical properties of the lumbar spine [2]. It is often of interest to compare differences in ranges of motion for lumbar spine segments between groups with varied age, degeneration, and back pain and such quantities can be determined with reference to the normal values. Table 2.1 displays normal ranges of lumbar segmental motion for males between 25-36 years.

The movement that occurs throughout loading on the vertebral column due to weight-bearing during upright posture or due to contraction of the longitudinal back muscles is known as axial compression. The annulus fibrosis, the tough circular ring of the intervertebral disc, and nucleus pulposus, the soft inner-core of the disc, bear the applied load and transfer it to the vertebral endplates [2]. The vertebral bodies around a disc draw closer to one another and the disc bulges in the radial direction [15–17]. The reason the vertebral bodies approximate is because the endplates arch away from the disc and the resulting deflection

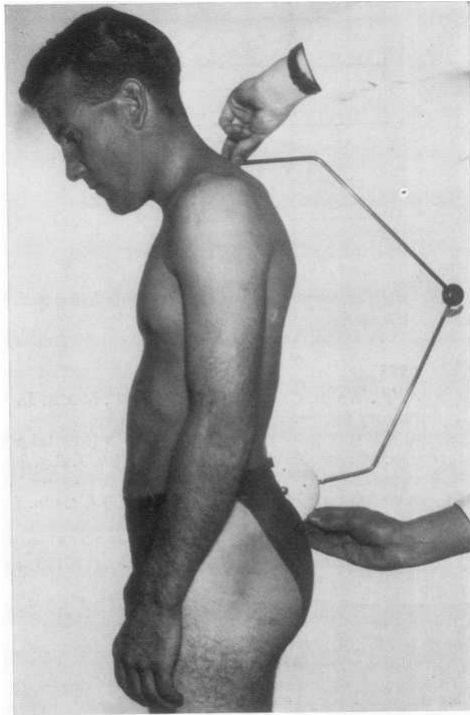


Figure 2.4: Example of a spondylometer, instrument consisting of two angled rods and a protractor, used to measure spinal mobility [12]

of each endplate is nearly half the displacement of the vertebrae [18]. Repetitively loading the lumbar intervertebral joints in compression may lead to fractures in the subchondral trabeculae and in one of the endplates [2] (Figure 2.5). Subchondral fractures can occur even after as few as 1000-2000 cycles from loads between 37-80% of the ultimate compression strength applied at 0.5 Hz [19]. Additionally, loads in the range of 50-80% of the ultimate stress can produce fractures in subchondral bone and vertebral bodies after less than 100 cycles [20].

Flexion involves the full lumbar spine leaning forward and straightening the lordosis curvature. During this movement, each intervertebral joint undergoes anterior sagittal rotation, as well as slight anterior translation until the zygapophysial (facet) joints are impacted. Compressive and shear forces are exerted on the intervertebral joints from the weight of the trunk and are proportional to the angle of the joint [2]. Mathematical analysis has been conducted in order to determine the concurrent contribution of different structures to resist

Table 2.1: Ranges of lumbar segmental motion in males 25-36 years old. (Based on Pearcy et al. 1984 [13] and Pearcy and Tibrewal 1984 [14]) [2]

Level	Mean range (measured in degrees, with standard deviations)						
	Lateral flexion		Axial rotation		Flexion	Extension	Flexion & extension
	<i>Left</i>	<i>Right</i>	<i>Left</i>	<i>Right</i>			
L1-2	5	6	1	1	8(5)	5(2)	13(5)
L2-3	5	6	1	1	10(2)	3(2)	13(2)
L3-4	5	6	1	2	12(1)	1(1)	13(2)
L4-5	3	5	1	2	13(4)	2(1)	16(4)
L5-S1	0	2	1	0	9(6)	5(4)	14(5)

lumbar flexion [22]. The findings relate only to resistance of anterior sagittal rotation and suggest that the approximate resistance distribution is as follows: the intervertebral disc contributes 29%, the supraspinous and interspinous ligaments contribute 19%, the ligamentum flavum contributes 13%, and the capsules of the facet joints contribute 39%. Repetitively loading the lumbar spine in flexion can lead to various lesions and fractures. Under pure bending, repetitive loading has minimal effect on the intervertebral joints [23]. However, repetitive bending under compression causes several different lesions in numerous structures. These lesions, ranging from lamellae buckling to radial fissures, are similar in nature to ones produced by pure compressive loading [2]. As a result of the facet joints resistance against forward translation during flexion, a bending force is applied on the pars interarticularis. Repetitively loading the inferior articular facets leads to failure of the pedicles or pars interarticularis (Figure 2.6).

During extension, bending backward in the opposite direction of flexion, the lumbar spine can be susceptible to a condition known interspinal osteoarthritis or “kissing spines” [25]. The condition occurs as a result of adjacent spinous processes colliding and crushing the interspinous ligament during lumbar extension. Because of the innervation of the spinous process periosteum and interspinous ligament [26], the condition can be considered a source

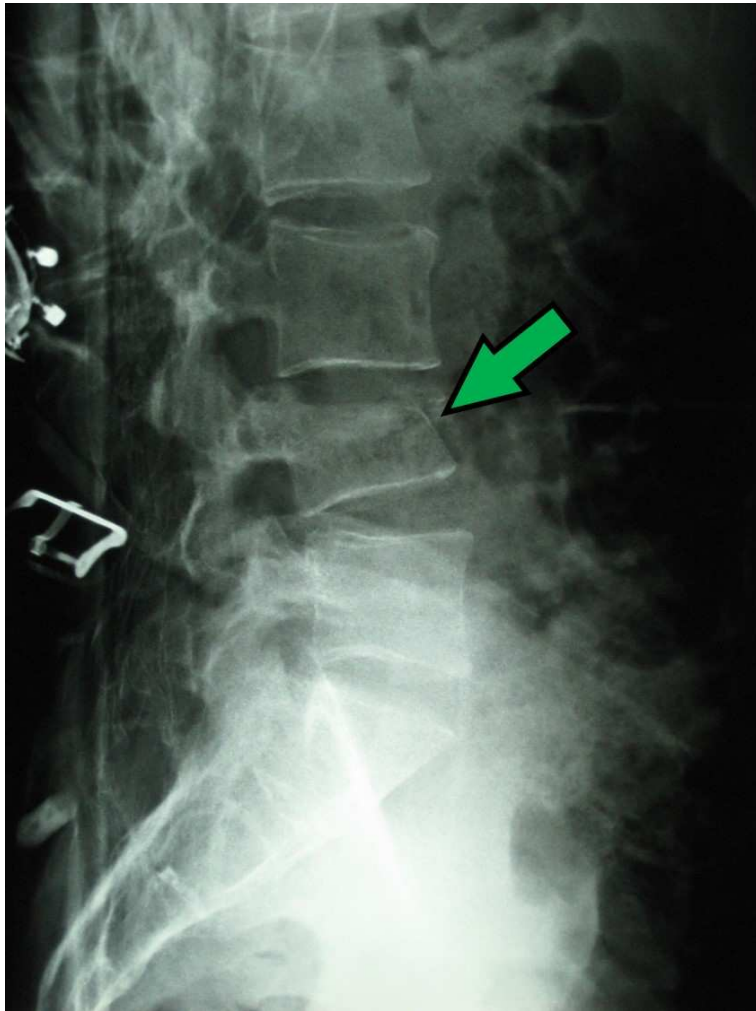


Figure 2.5: Lumbar spine compression fracture located at the L4 level [21]

of LBP. A similar condition to kissing spines can also disturb inferior articular processes in which the lamina is impacted during extension. If repeated extension injuries occur, the periosteum of the lamina can become irritated, causing lesions and pain [27].

Torsional motion of the intervertebral discs is known as axial rotation and as a result, the facet joints undergo impaction. The fibers of the annulus fibrosis angled towards the direction of rotation are strained while the other half is relaxed [2]. It has been calculated that the maximum range of rotation that an intervertebral disc can undergo without injury is approximately 3° and rotation past this range will result in collagen fibers beginning to experience micro-injury [16]. Extremely large forces are required to strain the intervertebral

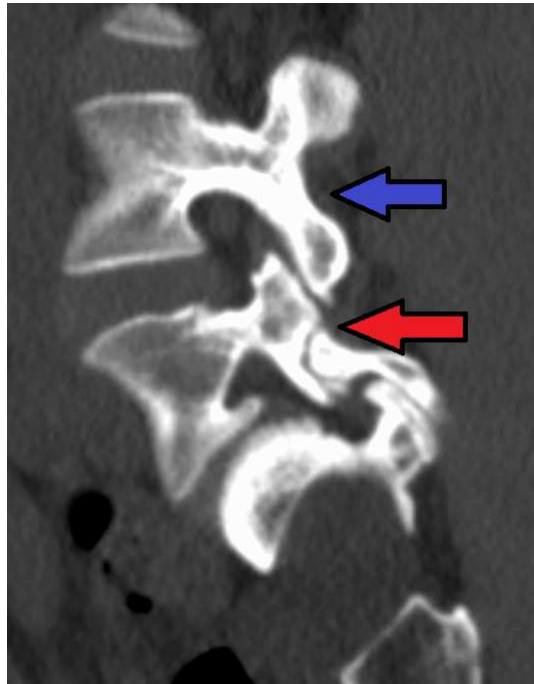


Figure 2.6: Lumbar spine bending fracture (blue arrow indicates intact pars interarticularis, red arrow indicates fractured pars interarticularis) [24]

disc past 3° and isolated discs fail at approximately 12° of rotation at the macroscopic level, suggesting that the range from $3 - 12^\circ$ of rotation describes continual microfailure until apparent macrofailure appears [28]. The elements that offer primary resistance to lumbar spine axial rotation are the facet joints, intervertebral disc, and supraspinous and interspinous ligaments. The tendency for elements to fail due to repetitive axial rotation varies depending on the initial range of motion. For example, if the intervertebral segment does not rotate past 1.5° it can withstand up to 10,000 rotations with no evident damage [2]. However, with a larger initial range of motion, segments can start to fail after 2,000-3,000 repetitions and sometimes even as few as 50 [29]. This failure is often seen as tears in the annulus fibrosis or fractures of the facet joints, laminae, or vertebral bodies. Due to the complexity of lateral flexion, which does not incorporate simple lumbar intervertebral joint movements, very few studies have analyzed this movement and determined corresponding mechanisms of fatigue [2].

2.2.2 Muscle function and conditions

Lumbar spine muscles can be potential sources of LBP because of their innervation. A common way to induce pain in healthy volunteers is with intramuscular injections of hypertonic saline [30]. This method has been proven through normal volunteers who received injections of hypertonic saline into their back muscles and as a result experienced LBP [31, 32]. Spinal muscles provide the main support for the body and allow for upright standing and various activities of daily living (ADL). Conditions involving spinal muscles can put the body in misalignment which in turn, can cause pain. It is controversial how to characterize disorders that influence the muscles of the lumbar spine, however, there are several that have been agreed upon as possible causes of LBP.

Scientists have come to a common agreement that chronic back pain, resulting from muscle pain, is due to muscle spasm [33]. This conclusion has been drawn from the suggestion that muscles develop irregular activity as a result of abnormal posture or articular pain and thus, become painful [2]. Ischaemia, the restriction of blood supply to muscles, is the main possible premise for this type of pain, but supporting evidence is unclear [33]. Additional experimental research must be collected in order to determine if the mechanisms of pain are from muscle attachment strain, ischaemia, or an alternative.

Through observations in the field of sports medicine, muscle strains have been believed to cause pain after intense exertion or abrupt stretching. Therefore, it can be hypothesized that such an injury could occur in the back muscles and cause LBP [2]. Failure at the myotendinous junction following muscles stretching against contraction has been commonly demonstrated in animal studies [34–36]. As a result, a lesion develops and is often acknowledged as a source of pain. There is no current evidence that directly supports lesions as a cause of back pain, however, it is not impossible to study further due to technology such as magnetic resonance imaging (MRI).

Sensitive areas in muscle are known as trigger points, or muscle knots, and are able to produce pain. They are identified as points with severe sensitivity in palpable bands of taut

muscle fibers [2]. Figure 2.7 shows a schematic of a trigger point complex. The taut fibers have a reduced width and contain swollen contraction knots within the trigger point. These points are believed to originate due to a reflex response to joint disease [37] or repetitive strain of the damaged muscle [38]. Studies have shown that the iliocostalis, longissimus, multifidus [39], and quadratus lumborum [40] muscles have been affected by trigger points, however, the diagnostic criteria is difficult to satisfy and it is unknown how frequently they cause LBP [2].

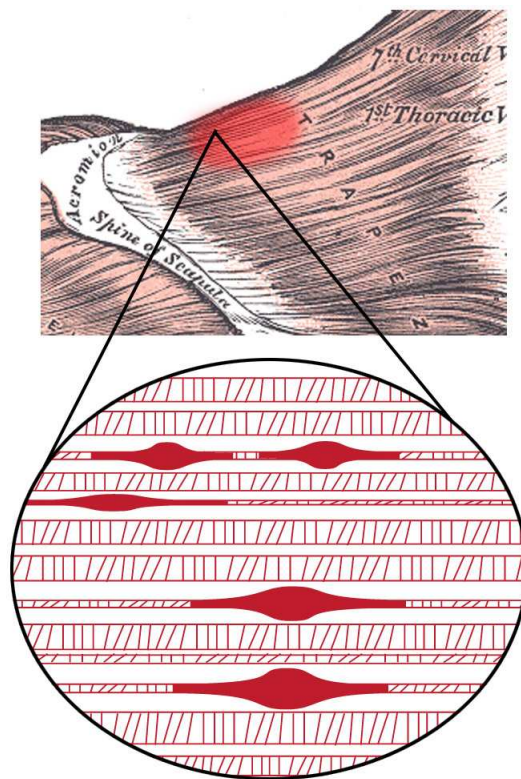


Figure 2.7: Schematic of a trigger point complex [41]

The concept of muscle imbalance refers to the ratio between the strength of agonist and antagonist muscles crossing a joint [42]. It is believed that deviations from normal muscle response in postural and phasic muscles, resulting in imbalance, can lead to pain [43]. Though many support the theory of muscle imbalance leading to LBP, it is unclear whether the pain emerges from one or more muscles or from resulting stresses on the affected joint [2]. The

theory was formed on the basis of clinical observation, but future research with objective confirmation must be conducted for the theory to be truly valid.

2.2.3 Tissue-level conditions

Because numerous elements within the biological mesoscale are innervated, many possible sources of pain are found within soft tissue. Namely, the lumbar fascia, dura mater, epidural plexus, sacroiliac and facet joints, spinal ligaments, and intervertebral disc are all probable sources of LBP. The thoracolumbar fascia creates a compartment around the back muscles. This has led to the idea that the back can be affected by compartment syndrome [44, 45], which is the concept that the back muscles enlarge during activity but their expansion is limited by the thoracolumbar fascia. Subsequently, pain can develop as a result of high strain in the fascia.

There are clinical similarities between patients with ligament injuries within the appendicular skeleton and patients with LBP. Thus, ligament sprain has been suggested as a possible source of back pain. The only two ligaments that have existing recorded data describing them as sources of back pain are the interspinous and iliolumbar ligaments [2]. Experimental stimulation of the interspinous ligament, which connect adjacent spinous processes, has been found to produce LBP [46]. Additionally, the interspinous ligaments are often degenerated centrally when analyzed post-mortem [47]. The iliolumbar ligament connects the tip of the L5 vertebral transverse process to the iliac crest's inner lip posteriorly and provides resistance against flexion, rotation, and lateral bending of the L5 vertebra [48–50]. During these movements the iliolumbar ligament can be susceptible to strain injury. Tenderness over the posterior superior iliac spine has been attributed to iliolumbar ligament sprain, but also the lumbosacral joint and back muscles, and it is unclear what specific disorder may be leading to pain [2].

Stressing the sacroiliac joint with injections of contrast medium was found to produce somatic joint pain in normal volunteers [51]. However, there is much uncertainty on mechanical disorders affecting the joint due to its small range of movement. Studies have

determined that sacroiliac joint pain can be diagnosed by using intra-articular injections of local anesthetic and about 15% of patients with chronic LBP were found to have sacroiliac joint pain [52, 53]. The pathology of this pain is unknown, but it can possibly be attributed to ventral capsular tears [53].

It has been established that the lumbar facet joints can produce LBP in normal volunteers. Particular patients have experienced relieved pain by anesthetizing one or more lumbar facet joints [54–58]. Though the prevalence is apparent for this pain, the pathology still remains unclear. The facet joints can be affected by various disorders, but the conditions have not been determined as the causes of pain in patients who have received anesthetic blocks [2]. Studies analyzing lumbar spine biomechanics have demonstrated that the facet joints can be injured by numerous movements. During extension, continued impact of an inferior articular process on the lower lamina causes the contralateral inferior articular process to rotate and capsular disruption of that joint [59]. This same damage can occur during continued axial rotation, as well as subchondral bone fractures, articular process fractures, and pars interarticularis failure [2]. A syndrome defined clinically as ‘acute locked back’ in which a patient is unable to straighten after bending forward because of severe pain is related to the facet joints. One theory is that one of the fibroadipose meniscoids within the joint is drawn out during flexion but is unable to re-enter the cavity during extension and thus causes pain from joint capsule swelling [60].

The most thoroughly studied and widely understood cause of chronic LBP is internal disc disruption (IDD). Out of all conditions, IDD has the strongest correlations between its formation, biophysics, and pain [2]. IDD is defined as degradation of the disc’s nuclear matrix with the existence of radial fissures directed from the nucleus to the annulus fibrosis (Figure 2.8). These fissures are given grades, from 1-4, depending on the extent at which they permeate the annulus [61]. IDD is a focal disorder in which the intervertebral disc may bulge, but the external boundary of the annulus stays intact. A disc with IDD exhibits decreased or non-existent nuclear stress and high stresses in the posterior annulus above normal, which

correlate well with reproducing pain through stimulation [62]. After repetitive compression loading, a vertebral end-plate fracture may occur which can result in healing or may induce IDD. If the degradation grows along a radial fissure for the full thickness of the annulus, disc herniation can occur [2]. It is currently not possible to diagnose IDD clinically, however, it is the single most common observable cause of chronic LBP, with a prevalence of at least 39% [63].

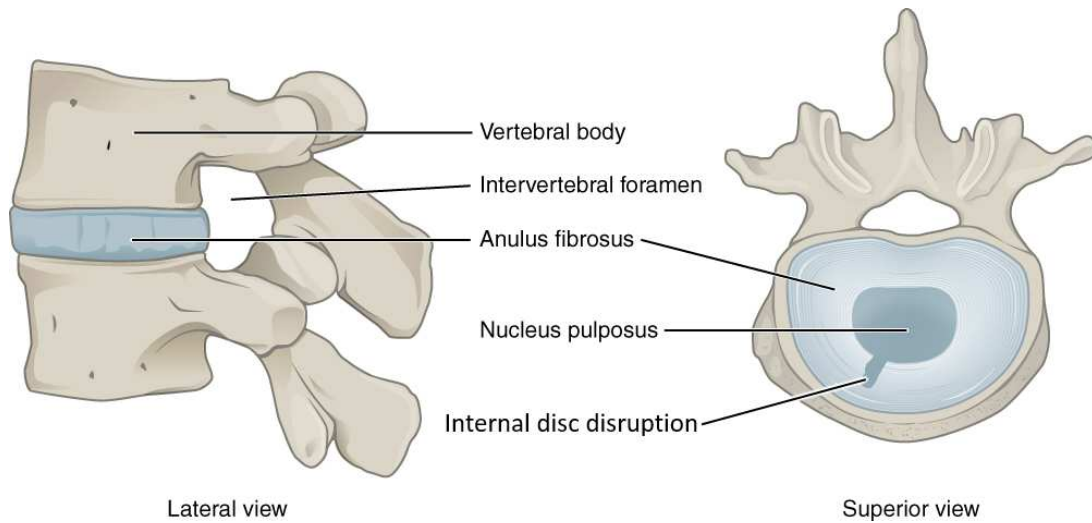


Figure 2.8: Example of a radial fissure in internal disc disruption (adapted from [64])

2.2.4 Summary

For decades, countless research analyses have been conducted in order to better understand the causes of LBP. Many concepts pose numerous elements of the lumbar spine as potential causes of pain. These theories must still be further tested, however, to determine the pathology of various conditions. A summary of the proposed sources of LBP and the extent to which they satisfy the postulates for a structure to be considered a source of LBP is shown in Table A.1.

2.3 Persons with a lower-limb amputation

In addition to the general population, LBP has been reported to affect up to 71% of persons with a lower-limb amputation (LLA) [4]. LBP is a major cause of secondary disabilities in the amputee population and nearly one-third of people with LLA and LBP report their pain as severe and that it hinders their ability to work and perform daily activities [5]. Though LBP has been known to significantly affect the LLA population, determination of the etiology and mechanisms of LBP remain controversial and inconsistent. Nonspecific LBP, which occurs in people with LLA, is proposed to involve many factors such as biomechanical, psychological, and social [65, 66]. In populations with abnormal spine kinematics, biomechanical factors play a large causal role [1].

Studies suggest that the increased prevalence of LBP in people with LLA is mainly due to kinematic and muscle asymmetries, rather than degenerative arthritis-related pain [3, 67]. People with a transfemoral amputation (TFA) and LBP were found to have increased transverse plane motion and extension of the lumbar spine compared to able-bodied controls [1]. During the stance phase of the prosthetic limb, most people with TFA laterally flex their trunk towards the amputated side [68] and throughout the gait cycle, show greater pelvic range of motion in the frontal and sagittal planes [69]. Decreased pelvic drop was reported to occur during the stance phase of the prosthetic limb and slight hip-hiking during swing phase of the prosthetic limb for people with a transtibial amputation (TTA) [70]. In order for kinematic asymmetries to exist, altered muscle recruitment must control the movement. People with TFA have increased muscle activity at the hip joint of the intact leg and people with TTA have increased activity of the hip extensors during early stance of both the intact and amputated legs compared to the corresponding leg on able-bodied controls [71]. An experimental study based on physical measures found significantly stronger back extensors in participants with TFA when compared to those with TTA, but significantly decreased back extensor muscle endurance in participants with TFA versus TTA [72]. A recent modeling study found that people with TTA had increased back extensor (erector

spinae) muscle forces on the intact side when compared to able-bodied participants [6].

Altered mechanical loads at various joints and in surrounding tissue result from the biomechanical asymmetries in people with LLA. Increased trunk lateral flexion toward the residual side is thought to help stabilize the body [70] but has been found to increase peak laterally-directed joint reaction forces and lateral bend moments by 83% and 41%, respectively, in prosthetic versus intact stance among people with TFA [73]. In the same study, peak anteriorly-directed reaction forces and extension moments were reported as 31% and 55% greater, respectively, among people with TTA versus able-bodied controls [73]. The asymmetric and increased mechanical loads at the low back that are found in people with LLA are potential causes of LBP, especially through repetitive abnormal loading.

2.4 Biomechanical modeling techniques

Validated computer models of the human musculoskeletal system are imperative to the field of biomechanics when certain parameters to be analyzed are difficult or impossible to measure *in vivo*. Musculoskeletal (MSM) and finite element (FE) modeling are conventionally accepted ways to model biological phenomena at the macro- and mesoscale, respectively. A newer, emerging technique in biomechanics is multiscale modeling which combines two or more scale levels in one simulation framework. The following sections describe the three modeling methods, studies of the spine, and current limitations.

2.4.1 Macroscale modeling

The components of the musculoskeletal system are fundamental in producing coordinated motion. However, there are important variables, such as joint contact and individual muscle forces, that are not measurable *in vivo*. The development of MSM has enabled scientists to produce computer generated dynamic simulations of human movement *in silico* to calculate estimates of values impossible to measure experimentally. Several of the established MSM platforms (both commercial and open-source) that are available currently include SIMM [74], AnyBody [75], and OpenSim [76]. Key capabilities of MSM are to analyze macroscale

biomechanics at the whole-body level in order to understand coordination of movement, the effects of various surgeries and pathologies, medical device design, and performance optimization.

The two main methods for generating MSM dynamic simulations in order to study muscle recruitment are the forward and inverse dynamics approaches [77]. Both methods apply the classical equations of motion, which can be written as:

$$M(q)\ddot{q} + C(q, \dot{q}) + G(q) = \tau \quad (2.1)$$

where $M(q)$ is the system mass matrix, q is the vector of generalized positions, \dot{q} is the vector of generalized velocities, \ddot{q} is the vector of generalized accelerations, $C(q, \dot{q})$ is the vector of Coriolis and centrifugal forces, $G(q)$ is the vector of gravitational forces, and τ is the vector of generalized forces (as described in the OpenSim documentation). The major difference between the two methods is that the forward dynamics approach applies muscle excitations or joint torques to a musculoskeletal model in order to produce movement and determine muscle force profiles while the inverse dynamics approach applies a known motion to a model in order to determine joint torques and muscle forces. The available input largely determines the MSM analysis method used. If electromyography (EMG) signals or joint torques are known, the forward dynamics method is utilized and if laboratory-recorded motion-capture data is available, the inverse dynamics method is employed. If all of these inputs are available, either or both methods may be used and results can be compared to one another.

Many whole-body musculoskeletal models define the head, arms, and torso as one lumped segment [78–80]. For studies analyzing the lower-extremity, this is an acceptable approximation. However, studies investigating the lumbar spine require more anatomical detail in the torso region in order to obtain realistic spinal loading and kinematic results. Musculoskeletal models of the lumbar spine have been developed and validated for various analyses, such as determining lumbar spine kinematics and estimation of muscle force profiles during walking, jogging, and trunk movements. The first published model of the human lumbar

spine was created in the AnyBody software and incorporated seven rigid segments (pelvis, 5 lumbar vertebrae, and lumped thoracic part), 154 muscles, and lumbar vertebral joints defined as 3-degrees-of-freedom (DOF) spherical joints [81]. Improving upon this was a lumbar spine musculoskeletal model created in the OpenSim platform which included the same seven rigid upper-extremity segments, 238 muscle fascicles, and lumbar vertebral joints defined as 6-DOF joints in which each lumbar vertebrae is assumed as a linear function of the coordinate of interest (flexion/extension, axial rotation, and lateral bending) (Figure 2.9) [82].

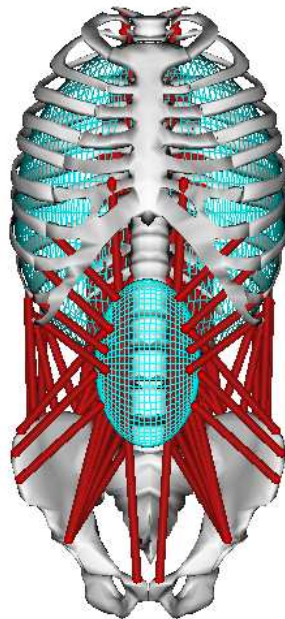


Figure 2.9: Musculoskeletal model of the human lumbar spine developed in OpenSim. Muscle wrapping objects are shown in blue mesh and muscle fascicles shown in red [82].

The lumbar spine MSM developed in OpenSim was further modified to incorporate 6-DOF stiffness at each intervertebral joint in order to obtain more accurate lumbar spine motion and loading [83]. Many musculoskeletal models do not incorporate stiffness of passive intervertebral structures, such as facet joints, ligaments, and intervertebral discs, which are thought to provide a crucial role on the muscle forces affecting joint loading [84]. Adding more detail to developed musculoskeletal models can provide better comparisons to *in vivo*

results. Established MSMs of the lumbar spine in both OpenSim and AnyBody have been adjusted to include the details of the thoracolumbar spine and articulating ribcage in an effort to more accurately predict spinal loading [84–86].

In order to test the sensitivity of lumbar spine loading to various anatomical parameters, Putzer et al. parameterized important vertebral features in a musculoskeletal model with several simulation cases and reported that vertebral body height and disc height had the largest effects on lumbar loading [87]. Another MSM study with a focus on spinal loading modeled an instrumented vertebral body replacement (VBR) in a whole-body MSM in order to determine the predictive power of the model to estimating in vivo spinal loads [88]. Currently, only one study has analyzed trunk and low back metrics using a musculoskeletal model of subjects with a unilateral, transtibial amputation. The study determined that people with unilateral TTA have different trunk-pelvis motion, greater L4L5 joint contact forces, and greater trunk-pelvis muscle forces compared to able-bodied controls [6]. The results provide a starting point for further work to discover a causative link between trunk-pelvis biomechanics and LBP among people with LLA.

2.4.2 Mesoscale modeling

If investigation of tissue-level stresses, strains, deformations, and loads is of interest, MSM approaches are no longer viable. Computer modeling of phenomena occurring at the mesoscale, or tissue-level, is most commonly performed with FE modeling and simulation. The FE method is a numerical analysis technique that utilizes integration for determining approximate solutions to boundary value problems for partial differential equations. There are many different FE modeling platforms available such as ABAQUS, ANSYS, LS-DYNA, and FEBio. Due to the difficulty in solving engineering problems at the mesoscale, FE analysis subdivides large systems into finite elements in order to obtain a solution. In biomechanics, this allows for soft tissues and joint contact surfaces to be modeled and analyzed.

Research groups have been analyzing spinal segments through FE modeling since the early 1990s [89–91]. The methods used to create these models have been developed over

time and currently, there is a standard method to create FE models of the lumbar spine, with differences lying typically in numerically defined values. The distinguishable features of the vertebral body are generally the cortical shell, cancellous core, bony endplates, and posterior bony elements. the distinguishable features of the intervertebral discs are generally the nucleus, annulus fibers, annulus ground substance, and cartilaginous endplates. In order to obtain realistic anatomical geometry, FE models of the human lumbar spine typically use geometry extracted from computed tomography (CT) or MRI scans. The majority of studies analyzing the lumbar spine define the vertebral cortical and cancellous bone as linear elastic isotropic material with Young's modulus of 12,000 and 10 *MPa* and Poisson's ratio of 0.3 and 0.2, respectively [92]. The bony and cartilaginous endplates and posterior bony elements are also defined as linear elastic isotropic materials with varying values for Young's modulus and Poisson's ratio. The articular facet joints are defined as unilateral frictionless connections that transmit only compressive forces with a designated initial gap [92].

The intervertebral disc plays an important role in load bearing and movement which is not captured in musculoskeletal modeling. In FE modeling, the nucleus pulposus, which contributes the most in compressive stiffness of the disc, is typically modeled as a fluid-like solid with linear elastic isotropic material properties. The annulus fibrosis, which provides protection for the nucleus pulposus, has frequently been defined as a linear elastic material with an isotropic matrix of tension-only elastic fibers [92]. The ligaments of the human body are behave nonlinearly [93], however, many FE studies of the lumbar spine have adopted a linear elastic definition [92]. A full FE model of the lumbar spine is shown in Figure 2.10 as a reference to the definitions previously described.

The anatomical geometry for FE models of the lumbar spine are typically taken from CT scans of a single subject. Several studies have explored this area further. Lalonde et al developed a free-form deformation (kriging) technique to deform a FE model of the lumbar spine to patient-specific geometry of 10- and 82-year-old asymptomatic spines [95]. Campbell et al developed a method to automatically create FE models of the lumbar spine from CT

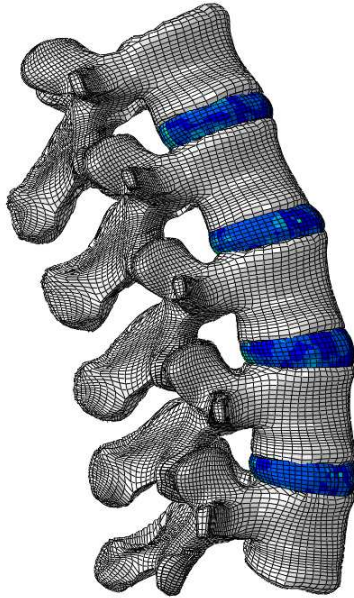


Figure 2.10: Finite element model of the human lumbar spine developed in ABAQUS. Bony elements are shown as white elements and intervertebral discs as blue elements [94].

geometry using a novel landmark identification approach [94]. Niemeyer et al parameterized geometric features of a FE model of the lumbar spine in order to determine which parameters account for the majority of variance of the model response [96].

One large reason for utilizing FE modeling to study the lumbar spine is that degeneration and pathological abnormalities can be simulated. Degeneration of the intervertebral disc is a common cause of LBP and understanding its biomechanical differences from asymptomatic discs is of great interest. Two previous studies have created FE models of the lumbar spine with varying degrees of intervertebral disc (IVD) degeneration in order to understand how degenerated IVDs affect intersegmental rotations, intradiscal pressures, and facet joint forces [97, 98]. *In vivo* loads on the lumbar spine are impossible to measure unless an instrumented device is surgically implanted. Still, these devices are typically implanted in symptomatic patients. FE modeling of the lumbar spine allows for estimation of these loadings on healthy and pathological subjects and an understanding of their biomechanical implications. Dreischarf et al reviewed estimated loads on the lumbar spine during various

postures determined from several *in vivo* and computational model studies [99] and Schmidt et al analyzed the response of the lumbar spine during regular ADL [100]. Rohlmann et al combined an *in vitro* experiment using an internal fixation device and computational FE study to estimate trunk muscle forces for upper body positions in the sagittal plane [101]. Schmidt et al analyzed the biomechanics of a FE model of a lumbar motion segment in pure and combined shear loads [102] and Dreischarf et al determined that caution must be used when estimating the compressive force in the lumbar spine from intradiscal pressure measurements [103].

Improvement of FE models of the lumbar spine should continue with new scientific findings and technologies. Several studies have explored methodologies to improve current computational models. Zander et al modeled the lumbar spine with the highest and lowest values for ligament stiffness from the literature separately in order to understand how ligament stiffness influences the biomechanics of a functional spinal unit [104]. Schmidt et al developed a calibration method to find the ideal material parameter combination of annulus fibers and ground substance for an FE model of a lumbar functional spinal unit [105]. Additionally, Schmidt et al also conducted a review study on what FE modeling studies of lumbar IVDs have found over the past four decades, such as the roles of its constituents, its biodynamics, and its transport [106]. Dreischarf et al compared eight published, validated FE models of the lumbar spine and determined that the combination of models provides an improved prediction in estimating the response due to loading [107].

2.4.3 Multiscale modeling

Biological phenomena span across many spatial scales and in order to understand how a higher level scale influences a lower level scale, and vice versa, MSM and FE methods are no longer valid individually. Techniques of modeling multiple spatial scales simultaneously, defined as multiscale modeling, are required to understand the integrative nature of system levels. These methods have been in existence for many years in areas such as chemistry, mathematics, and material science and have also been employed previously in the field of

biomechanics for various parts of the human body. In the musculoskeletal system, studies of pain in which the etiology is multi-factorial or relative to locomotion necessitates the need for a multiscale modeling approach. Disorders and injuries that involve the interaction of muscle activation and soft tissue deformation, such as diabetic foot ulceration, require understanding the relation between macro- and mesoscale biomechanics. Mechanism of noncontact anterior cruciate ligament (ACL) injury could also be better understood through a multiscale approach by modeling detailed muscle wrappings and activations, as well as accurate interaction with surrounding tissue [108]. Utilizing multiscale modeling techniques to better understand low back pain for persons with a lower limb amputation is thus a similar concept.

Several groups have reviewed the large need for further development of multiscale modeling in computational biomechanics, as well as addressed past work and current limitations [108, 109]. Tawhai et al. recognized current tools that can be used for multiscale biomechanics analyses such as open-source musculoskeletal [76] and finite element [110] modeling programs and atlasing projects such as the Allen Brian Atlas [111]. Priorities in multiscale computational biomechanics determined by Tawhai et al. are sharing of models, development of a standard format, and dissemination of a solution database [108]. Ateshian et al. also addressed several challenges that must be overcome in what they term “integrative biomechanics.” They also propose the development of supporting databases, as well as *in vivo* measurements of structure and function that are higher spatially and temporally resolved and building a close partnership between engineers, biomedical scientists, and clinicians to promote patient-specific treatment [109].

Despite the numerous challenges and limitations, multiscale biomechanical modeling has been employed throughout the human body. Halloran et al. reviewed the need for multiscale modeling in studying cartilage mechanics and proposed a simulation structure in which muscle forces and joint movement from musculoskeletal modeling can be used to inform a finite element model of the whole knee joint, the cartilage stress-strain from the joint FE

model can be used to inform a microstructural FE model of soft tissue, and the chondrocyte stress-strain from the tissue FE model can be used to inform a microscale model of tissue fiber. This pathway, used with feed-forward coupling, can provide potential causes of cartilage damage and mechanical catalysts at the multiscale level on chondrocytes [112]. Another study utilized multiscale modeling to determine if and how the lines of action of hip joint muscles cause edge loading on a well-designed and well-positioned hip replacement. The framework consisted of extracting muscle origins, insertions, and forces from a musculoskeletal model in OpenSim and using them to simulate a finite element model of a hip joint in Matlab as shown in Figure 2.11 [113]. Phillips et al. also utilized musculoskeletal and finite element modeling in a multiscale framework. A structural optimization routine was developed to predict the structure of the femur during two loading cases with a musculoskeletal model of the lower limb and a FE model of the femoral segment with cortical and trabecular bone modeled according to their structural properties [114].

Few studies have modeled the human spine using a multiscale approach. McDonald et al. developed a multiscale FE model of the osteoporotic lumbar vertebral body to study the mechanics of vertebral compression fracture at the apparent and microstructural levels. The model consisted of the whole vertebral body using linear shell elements and the microstructural internal trabecular bone core using a lattice structure determined from micro-CT scans [115]. McDonald's multiscale model was implemented completely in a finite element framework, while Han et al. developed a multiscale model entirely in a musculoskeletal framework. The purpose of their work was to add short segmental muscles, lumbar ligaments, and disc stiffnesses to an existing musculoskeletal model to determine what role passive soft tissues have in spinal loading [84]. Although their model lacks the detail that FE models provide, the model is still considered multiscale since it incorporates bones and muscles at the macroscale and disc stiffnesses and lumbar ligaments at the mesoscale. Instead of creating a multiscale model within one simulation framework, Zhu et al. incorporated both FE and musculoskeletal modeling. The purpose of the study was to determine the effects of the definition of the

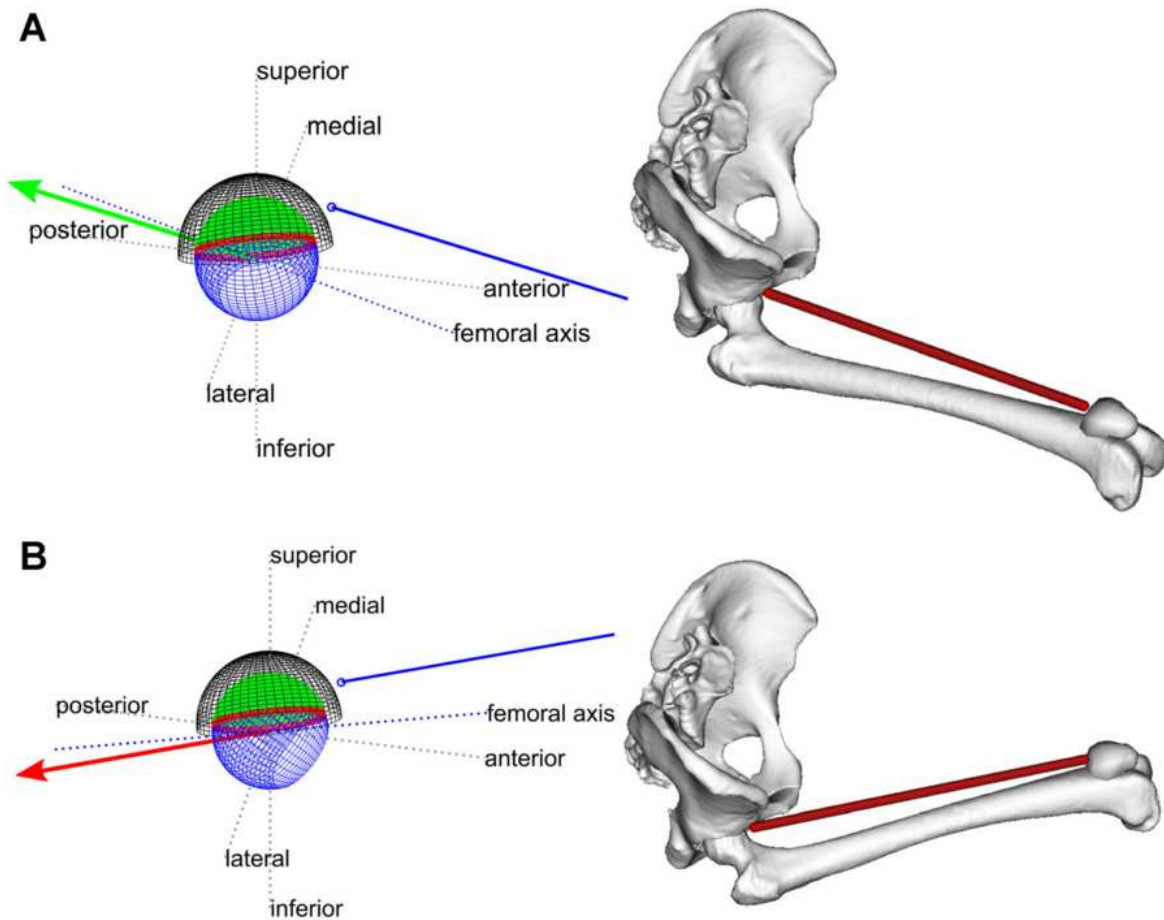


Figure 2.11: Diagrams indicating the line of action of the rectus femoris (blue line) and its hip joint reaction force (green/red arrow). The left column shows the discretized hip joint FE model and the right column shows representative positions from the musculoskeletal model [113].

center of rotation and the elasticity of bony structures when combining a musculoskeletal model and FE model of the spine. Anatomical geometry was adjusted to match in both models. Intervertebral rotations of 20 deg flexion and 10 deg extension were applied to the musculoskeletal model and muscle forces determined through optimization. These muscle forces were transferred to the FE model and the resulting motion (intervertebral rotations) were observed. Various deviations of intervertebral rotations occurred between models and Zhu et al. concluded that the fixed centers of rotation and the rigidity of the bony structures used in musculoskeletal models will often lead to different intervertebral rotations when es-

estimated muscle forces are used with elastic FE models [116]. Although not specific, this is an important finding for studies that involve using motion-captured kinematics to estimate muscle forces that drive a FE model to determine tissue stresses and strains. Future work in multiscale modeling of the spine must ensure convergence between all scale levels and simulation platforms.

CHAPTER 3

DEVELOPMENT OF A MULTISCALE MODEL OF THE LUMBAR SPINE: APPLICATION FOR PERSONS WITH A TRANSTIBIAL AMPUTATION DURING SIT-TO-STAND

A manuscript to be submitted to *IEEE Transactions on Biomedical Engineering*
or *Journal of Biomechanics*

Jasmin D. Honegger¹, Jason A. Actis², Deanna H. Gates³, Anne K. Silverman⁴,
Ashlyn H. Munson⁵, and Anthony J. Petrella⁶

3.1 Abstract

Persons with a transtibial amputation (TTA) have an increased prevalence of low back pain (LBP) compared to the general population, which is related to biomechanical causes. However, how different kinematics at the whole-body level affect potential sources of pain at the tissue-level remains unclear. A multiscale model was constructed by combining musculoskeletal and finite element (FE) models of the lumbar spine to characterize the interconnectivity between the two scales without invasive measurements. Kinematic and kinetic data were collected from people with ($n = 4$) and without ($n = 4$) TTA during sit-to-stand. An inverse kinematics solution was determined for an eight-segment model with 19 degrees of

¹Master's candidate at Colorado School of Mines (Dept. of Mechanical Engineering), Primary researcher and author, Responsible for musculoskeletal model development, multiscale model development, output and statistical analysis

²Master's candidate at Colorado School of Mines (Dept. of Mechanical Engineering), Responsible for musculoskeletal model development, experimental data processing

³Assistant professor at University of Michigan (School of Kinesiology), Responsible for experimental study design, experimental data collection

⁴Associate professor at Colorado School of Mines (Dept. of Mechanical Engineering), Responsible for experimental study design, musculoskeletal model development

⁵Teaching associate professor at Colorado School of Mines (Dept. of Applied Mathematics & Statistics), Responsible for statistical analysis

⁶Associate professor at Colorado School of Mines (Dept. of Mechanical Engineering), Corresponding author, Responsible for multiscale model development

freedom, which is then input with ground reaction forces and a musculoskeletal model into a static optimization framework that solved for muscle recruitment. Geometry, muscle attachment locations, muscle forces, joint contact forces and moments from the torso-L1 joint, and L5 vertebra orientation were transferred from the musculoskeletal model to the FE model. Lumbar spine kinematics were similar between models with the greatest discrepancy (12.89° in flexion) occurring at the moment of lift-off. Participants with TTA had different lumbar kinematics compared to able-bodied participants (e.g., more flexed posture) throughout the motion. Regression models predicted more than 50% of the variance in each tissue-level metric for annulus fibrosis von Mises stress vs. flexion/extension, facet joint contact force vs. axial rotation, and intradiscal pressure vs. flexion/extension for all participants. The multiscale model provides insight into the interconnectivity between scale lengths and can extend to use with other activities to inform treatment of LBP.

3.2 Introduction

Low back pain (LBP) is a common problem in the general population and has an increased prevalence among people with a lower-limb amputation (LLA) [3, 4]. For many people with LLA, LBP is known as a secondary condition commonly linked with altered movement strategies as a result of adaptation to limb loss [5]. The primary causes of LBP for people with LLA are related to biomechanical consequences such as whole-body kinematic and muscle asymmetries [1]. The sources of LBP are known to exist at the tissue-level such as within the intervertebral discs or facet joint capsules [2]. However, the current standard of care to treat people with LLA and LBP is physical therapy, which is an intervention at the whole-body level. There is a need to bridge the gap between determining the source of pain at the tissue-level and the biomechanical cause of pain at the whole-body level to better understand mechanical LBP and the appropriate therapeutic intervention.

Computational modeling techniques allow for estimation of biological quantities that are difficult or impossible to measure *in vivo*. Dynamic rigid-body simulations of human movement can be performed with musculoskeletal models to estimate muscle forces and joint

loading. Finite element (FE) models can be used to simulate certain regions of the body and estimate tissue-level mechanics. Previous musculoskeletal modeling studies have tested the sensitivity of lumbar spine loading to various anatomical parameters [87], determined the predictive power of a musculoskeletal model to estimate in vivo spinal loads from vertebral body replacements [88], and analyzed low back kinematics and loading for people with a unilateral transtibial amputation (TTA) during walking [6]. Finite element modeling studies have primarily focused on the effects of ligament stiffness [104], annulus fiber and ground substance material parameters [105], and other material properties on lumbar spine biomechanics. Separately, musculoskeletal and FE modeling techniques have certain limitations such as lack of constitutive detail in musculoskeletal models and computational expense in FE models.

Multiscale modeling involves analyzing models that span multiple spatial scales in one simulation framework. These models allow for the investigation of the coupling and interconnectivity between spatial scales. Few studies have modeled the human lumbar spine using a multiscale approach. McDonald et al. developed a multiscale FE model of the osteoporotic lumbar vertebral body to study the mechanics of vertebral compression fracture at the apparent and microstructural levels [115]. Another study added short segmental muscles, lumbar ligaments, and disc stiffness to an existing musculoskeletal model to determine what role passive soft tissues have on spinal loading [84]. Zhu et al. incorporated both musculoskeletal and FE modeling techniques in a multiscale model to determine the effects of the centers-of-rotation and elasticity of bony structures on intervertebral kinematics during 20° flexion and 10° extension [116].

The sit-to-stand movement is a common daily activity that is often used to assess lower-limb strength in the elderly and in populations with lower-limb deficiencies [117]. Previous studies have found that people with LBP have motion compensation and altered load sharing strategies such as straight leg raise, altered moments and powers acting across the lumbar spine and hips [118], and reduced sagittal-plane mobility [119] during sit-to-stand when

compared with asymptomatic individuals. Additionally, lumbosacral joint moments and powers have been found to be significantly larger among people with a unilateral transfemoral amputation as compared to able-bodied participants [120]. These studies provide helpful insights on whole-body metrics for patients with LBP and people with LLA during sit-to-stand, but to our knowledge, no previous study has combined the benefits of musculoskeletal and FE modeling techniques to investigate tissue-level metrics commonly associated with LBP during dynamic movements, such as sit-to-stand.

The purpose of this study was to create a multiscale model of the human lumbar spine to identify and characterize the interconnectivity between whole-body biomechanics and tissue-level metrics leading to LBP for people with a unilateral transtibial amputation (TTA) during sit-to-stand. We hypothesized that: 1) People with TTA would have greater ranges of trunk-pelvis motion than able-bodied participants; 2) People with TTA would have greater peak von Mises (vM) stress in the annulus fibrosis, greater peak facet joint contact forces, and greater average intradiscal pressure than able-bodied participants; 3) Maximum lumbar spine lateral bending would correlate with peak annulus fibrosis vM stress; 4) Maximum lumbar spine axial rotation would correlate with peak facet joint contact force; and 5) Increased lumbar spine flexion would correlate with greater average intradiscal pressure.

3.3 Methods

3.3.1 Multiscale model development

A whole-body musculoskeletal model with lumbar spine fidelity was developed in OpenSim 3.3. The model includes detail of the lumbar spine and torso from [82], the lower extremity from [78–80, 121, 122], muscle strengths from [85], and body mass distribution from [123]. Muscles were represented with 294 Hill-type musculotendon actuators with force-length-velocity properties [124]. The model contains 18 body segments (torso, five lumbar vertebrae, sacrum, pelvis and left and right femur, shank, calcaneus, talus, and toes) and 19 degrees of freedom (DOF) (subtalar and metatarsophalangeal joints locked) with the motion of the five lumbar intervertebral joints constrained as a linear function of the total

trunk-pelvis motion [82]. Another version of the model was created to represent a person with TTA by removing the twelve muscles crossing the amputated leg ankle joint, decreasing the residual shank mass, and shifting the residual shank center-of-mass location proximally [125]. Estimates of L4-L5 loading and muscle activations from the musculoskeletal model and static optimization framework have been validated with *in vivo* measurements of intradiscal pressure and surface electromyography during planar trunk-pelvis movements [126].

A validated FE model of the lumbar spine created in Abaqus/Standard [127] replaced the L1-L5 geometry of the musculoskeletal model (Figure 3.1a). The FE geometry was registered to the nominal configuration of the musculoskeletal lumbar spine using the Iterative Closest Point algorithm. Lumbar spine muscle attachment locations were obtained using a plugin developed for OpenSim [113, 114] and were transferred from musculoskeletal model to the FE model (Figure 3.1b). The fixed centers-of-rotation for each musculoskeletal model intervertebral joint were implemented in the FE model to constrain the motion of the joints to 3 rotational DOF (Figure 3.1c).

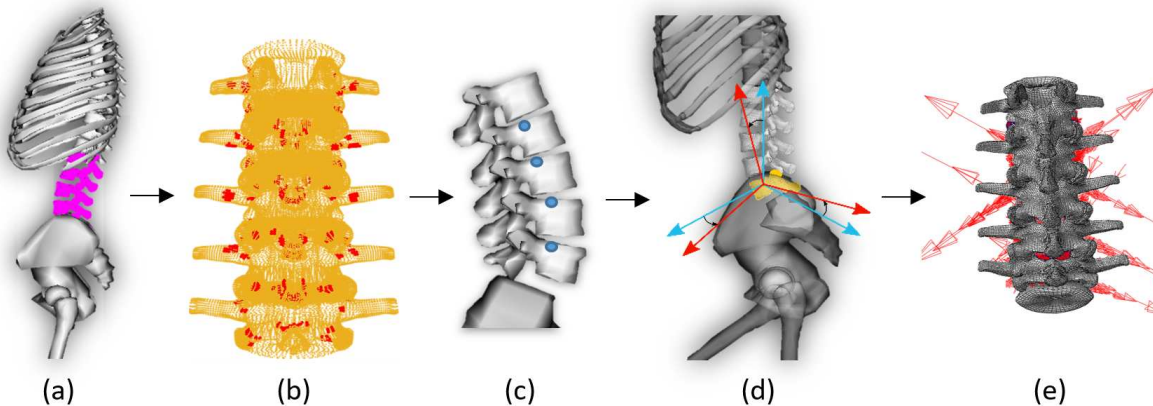


Figure 3.1: Workflow of the multiscale model development: (a) Scaling and registration of the FE model geometry to the musculoskeletal model, (b) determination of lumbar spine muscle attachment locations, (c) application of fixed centers-of-rotation in each FE model intervertebral joint, (d) prescription of L5 rotational boundary conditions for match the experimental motion, and (e) application of joint contact forces and moments for the torso-L1 joint and lumbar spine muscle forces to the FE model.

3.3.2 Experimental protocol

Four people without an amputation (able-bodied, 1M/3F, 23.3 ± 2.9 years, 1.66 ± 0.06 m, 65.9 ± 9.3 kg) and four people with a unilateral transtibial amputation (TTA, 4M, 45.5 ± 14.8 years, 1.84 ± 0.02 m, 99.4 ± 15.3 kg) provided informed consent to participate in the protocol approved by an Institutional Review Board. No participant had more than minimal LBP as indicated by the Modified Oswestry Low Back Pain Questionnaire [128]. All participants performed five self-paced sit-to-stand trials, starting from seated with hips, knees, and ankles at 90° of flexion and feet hip-width apart on separate force plates recording at 1200 Hz. Participants were instructed to keep arms folded across the chest for the duration of the motion. Kinematics were collected at 120 Hz using a 20-camera motion capture system and a full-body marker set including reflective markers placed at C7, T8, xyphoid process, and bilaterally at the acromion, posterior superior iliac spine (PSIS), anterior superior iliac spine (ASIS), iliac crest, and greater trochanter.

3.3.3 Simulation workflow

Kinematics and ground reaction forces (GRFs) were low-pass filtered with a bidirectional 4th-order Butterworth filter with cutoff frequencies of 6 Hz and 10 Hz, respectively. The portion of sit-to-stand data used for the simulations was from the moment of lift-off from the seat. An inverse kinematics solution was determined using least-squares optimization algorithm with an eight-segment model [129] in Visual3D and input to the musculoskeletal model. A residual reduction algorithm was performed in OpenSim to reduce residual forces and moments and improve dynamic consistency between ground reaction forces and accelerations estimated from the measured marker kinematics and Newton's 2nd Law. The orientation of the L5 vertebra at each increment of the motion was determined from the musculoskeletal model and applied to the FE model (Figure 3.1d). A custom OpenSim plugin was used [113, 114] to obtain the unit vector of each muscle at each increment in time. Using a static optimization method that minimized the sum of muscle activations

squared, the force developed by each muscle was estimated at each instant in time during the motion. These unit vectors and forces were then applied to the FE model as loading conditions. Joint contact forces and moments were also determined for the joint between the torso and L1 in the musculoskeletal model and applied to the FE model for dynamic consistency (Figure 3.1e).

3.3.4 Output and statistical analysis

To evaluate the accurate transfer of muscle forces and consistency of the models at the two length scales, FE output kinematics were compared to OpenSim input kinematics. The tissue-level metrics extracted from the FE simulations were contact force at the facet joints, vM stress in the annulus fibrosis, and fluid cavity pressure within the nucleus of the intervertebral discs. All hypotheses were tested by comparing participants with and without TTA using unpaired t-tests ($\alpha = 0.05$). Scatter plots of each lumbar spine rotational degree of freedom (DOF) versus each tissue-level metric were generated to determine the most appropriate regression model for each comparison (Figure 3.2). To account for the existence of possible asymmetries, right-side facet joint contact forces were adjusted to negative values and added to left-side contact forces for all DOF (denoted as “with +/−”). For flexion/extension, actual facet joint contact forces from the left and right sides were added together to capture the total magnitude of contact force at each increment in the motion (denoted as “without +/−”). Only peak values of annulus fibrosis vM stress were extracted at each time increment for analysis.

Based on the relationship scatter plots (Figure 3.2), the regression models chosen were: logarithmic for intradiscal pressure vs. flexion/extension and vM stress vs. flexion/extension; linear for facet joint contact force vs. flexion/extension (with +/−); quadratic for intradiscal pressure and annulus fibrosis vM stress vs. axial rotation and lateral bending and facet joint contact force (‘without +/−’) vs. flexion/extension; and cubic for facet joint contact force (with +/−) vs. axial rotation and lateral bending. Average curves from participant trials were used for the regression analyses. Residual versus fits plots were generated for each

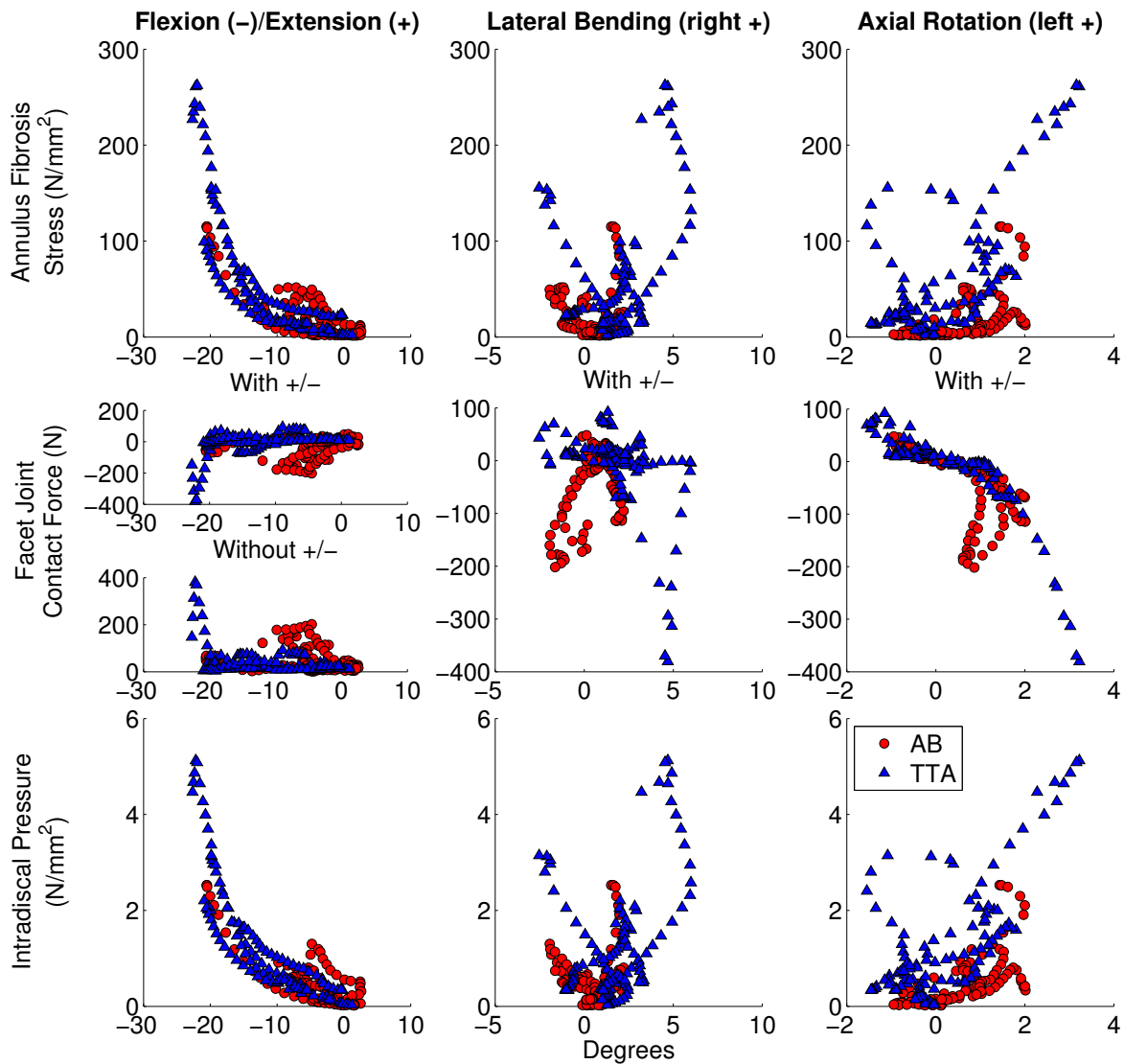


Figure 3.2: Scatter plots of each lumbar spine rotational DOF during sit-to-stand versus each tissue-level metric to determine the most appropriate regression model for each comparison for able-bodied (AB) participants and participants with TTA. Facet joint contact force plots labeled as “With +/-” and “Without +/-” to denote force calculation method.

regression comparison in order to ensure that the correlation and assumption of equal error variance was reasonable. Normal probability plots were also generated for each regression to determine if each data set was normally distributed.

3.4 Results

The output kinematics from the FE model compared well to the input kinematics from OpenSim (Figure 3). For all DOF, the greatest difference was 12.89° and occurred at the moment of lift-off in the sagittal plane. The maximum differences in kinematics for lateral bending and axial rotation were 0.77 and 0.78 degrees, respectively. Participants with TTA had greater average ranges of trunk-pelvis motion in the sagittal and frontal planes compared to able-bodied participants (Figure 4) of 9.54 and 1.57 degrees, respectively. In the transverse plane, able-bodied participants had a greater average range of motion than participants with TTA by 1.42 degrees. However, no significant differences were found in ranges of trunk-pelvis motion between participants with and without TTA.

The means of peak annulus fibrosis vM stress and facet joint contact force were not different between able-bodied participants and participants with TTA (Table 3.1). Only the average intradiscal pressure at the L3-L4 and L4-L5 levels and averaged across levels was different between participant groups ($p = 0.0449, 0.0269, \text{ and } 0.0396$, respectively). However, all tissue-level metrics at all lumbar levels had greater mean values for participants with TTA compared to able-bodied participants.

None of the residuals versus fits plots showed indication of incorrect mean structure and all points were randomly dispersed. Only the regressions for annulus fibrosis vM stress vs. flexion/extension, facet joint contact force vs. axial rotation, and intradiscal pressure vs. flexion/extension had a normal distribution. Due to this finding and the results from the relationship scatter plots (Figure 3.2) and regression analyses (Table 3.2), annulus fibrosis vM stress vs. flexion/extension was selected for further analysis instead of annulus fibrosis vM stress vs. lateral bending (Figure 3.5). All p -values were less than 0.000 and simple R^2 values were used because adjusted R^2 values differed by 0.008 (± 0.004). Overall, the regression equations matched the dependent tissue-level metrics well (Table 3.2). All R^2 values greater than 0.7 occurred in the regressions for annulus fibrosis vM stress vs. flexion/extension and axial rotation, facet joint contact force vs. axial rotation, and intradiscal pressure vs.

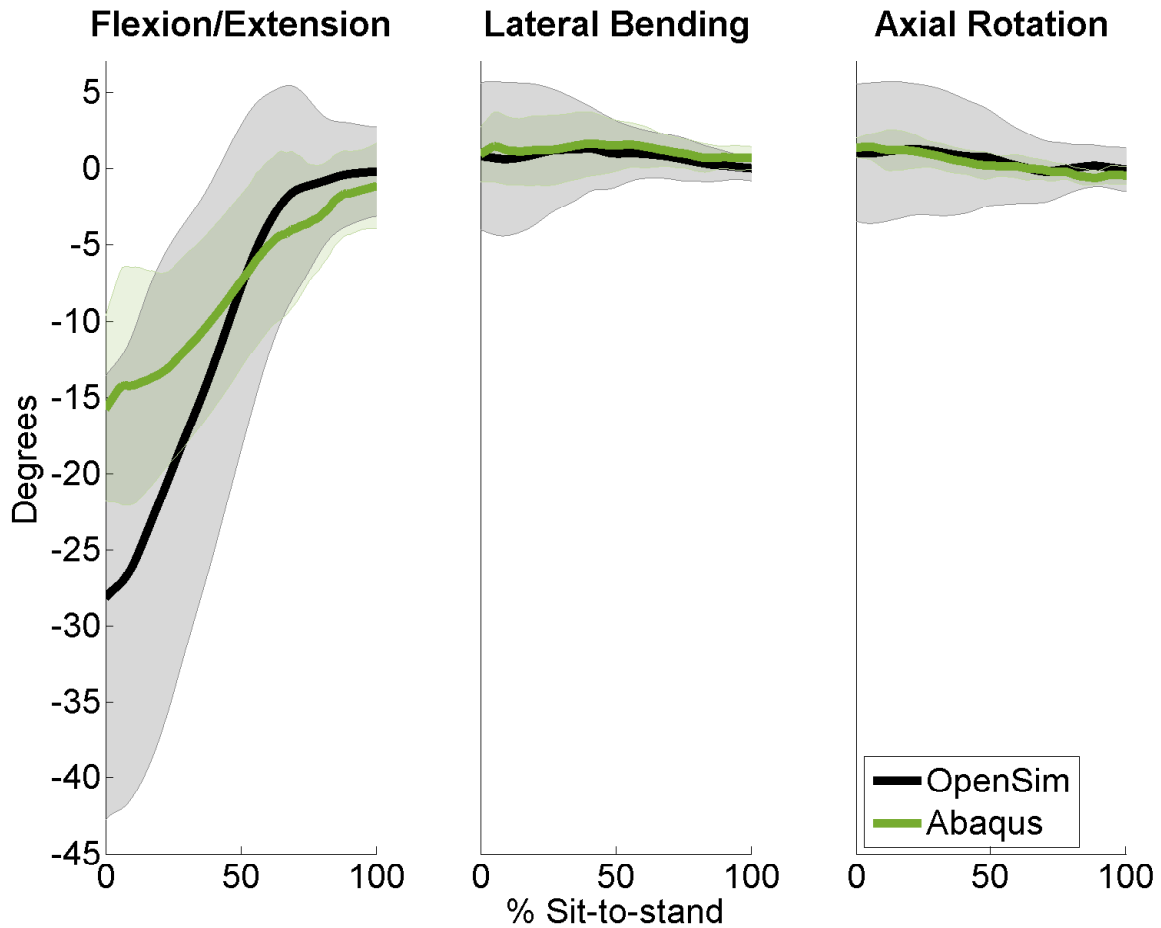


Figure 3.3: Multiscale lumbar spine kinematic evaluation (mean \pm 1 standard deviation) for all participants between the OpenSim input (black curves) and Abaqus output (green curves) kinematics.

flexion/extension. Participants with TTA had higher R^2 values than able-bodied participants for all regressions except for facet joint contact force vs. lateral bending. Regression models fit well to the normally distributed data for each participant group (Figure 3.5).

3.5 Discussion

The purpose of this study was to create a multiscale model of the human lumbar spine to identify and characterize the interconnectivity between whole-body biomechanics and tissue-level metrics leading to LBP for people with a unilateral transtibial amputation (TTA) during sit-to-stand. In this multiscale framework, the FE model played the role of sensor to deliver

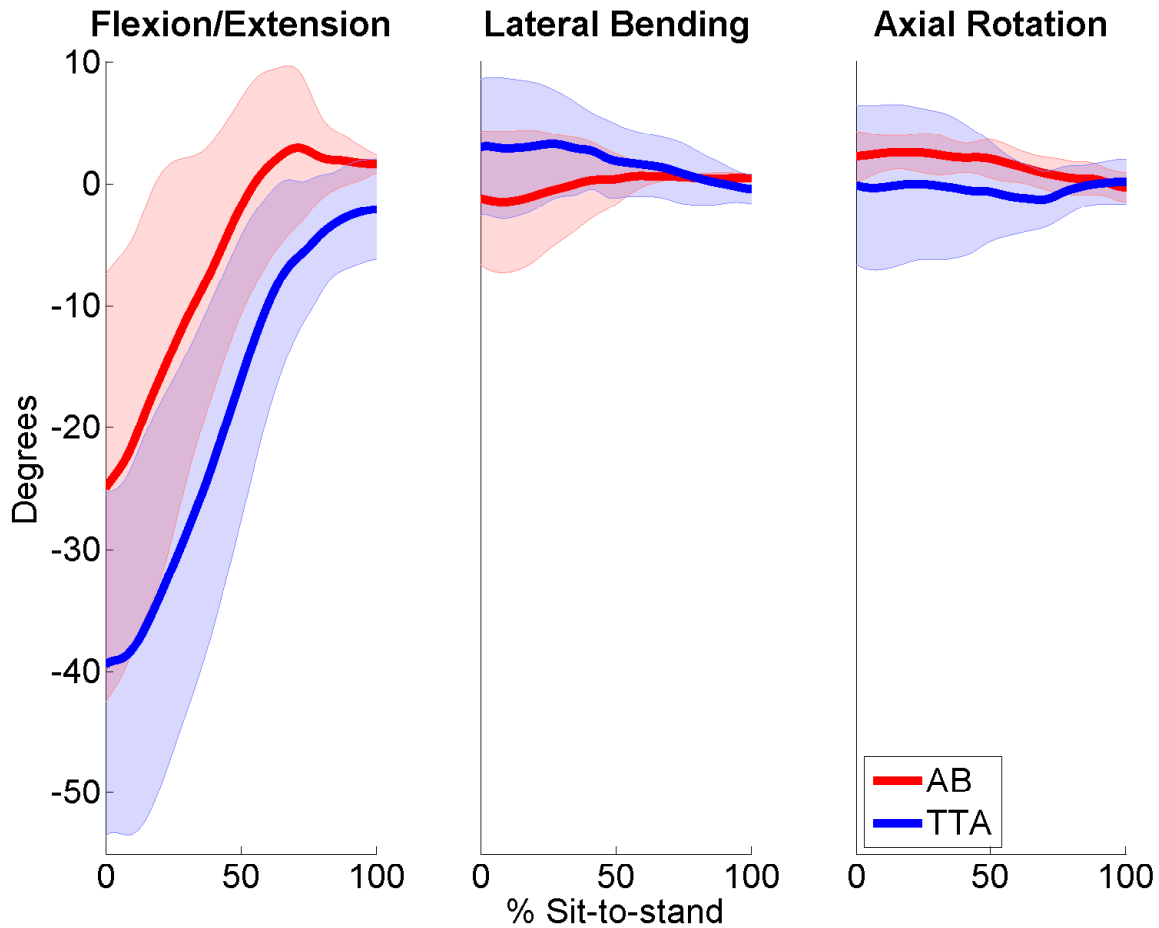


Figure 3.4: Trunk-pelvis kinematics (mean \pm 1 standard deviation) for participants with TTA (blue curves) and able-bodied (AB) participants (red curves) determined by inverse kinematics within the musculoskeletal model framework.

tissue-level metrics (annulus fibrosis vM stress, facet joint contact force, intradiscal pressure, etc.) not represented by the musculoskeletal model. The lumbar spine kinematic comparison to evaluate the transfer of loads from the musculoskeletal to FE model was good, with the largest discrepancy was the FE model under-predicting flexion by 12.89 degrees at the initiation of sit-to-stand. This disagreement may be due to the difference in control scheme between the two models, where the whole-body musculoskeletal model was displacement-controlled and the tissue-level FE model was force-controlled. In addition, utilization of bushing elements at the intervertebral joints in the musculoskeletal model [83, 130] with

Table 3.1: Mean (\pm standard deviation) of peak annulus fibrosis vM stress, peak facet joint contact force, and average intradiscal pressure for participants with TTA and able-bodied participants at each lumbar spine level and averaged across levels ($\alpha = 0.05$; significant difference denoted by *).

Tissue-level metric	Lumbar level	Participants with TTA	Able-bodied participants	<i>p-value</i>
Peak annulus fibrosis vM stress (MPa)	L1-L2	57.54 (19.37)	51.98 (38.79)	0.8062
	L2-L3	190.46 (117.27)	61.90 (59.37)	0.0982
	L3-L4	180.77 (113.66)	60.67 (64.74)	0.1160
	L4-L5	212.55 (124.57)	129.08 (65.95)	0.2811
	AVG	154.54 (88.28)	68.45 (44.15)	0.1317
Peak facet joint contact force (N)	L1-L2	21.24 (35.43)	9.19 (16.39)	0.3946
	L2-L3	40.55 (59.72)	20.43 (28.51)	0.4044
	L3-L4	41.47 (59.25)	24.72 (34.79)	0.5017
	L4-L5	45.38 (57.18)	25.03 (31.79)	0.5007
	AVG	35.25 (51.24)	19.67 (27.42)	0.4609
Average intradiscal pressure (MPa)	L1-L2	0.25 (0.12)	0.21 (0.21)	0.7778
	L2-L3	1.53 (1.03)	0.43 (0.34)	0.0886
	L3-L4	1.28 (0.68)	0.35 (0.29)	0.0449*
	L4-L5	2.10 (0.77)	0.91 (0.27)	0.0269*
	AVG	1.29 (0.59)	0.48 (0.20)	0.0396*

Table 3.2: Results from the regression analyses for each participant group (ALL: all participants, AB: able-bodied participants, TTA: participants with TTA). $R^2 \geq 0.7$ are shown in bold.

Tissue-level metric		Flexion/Extension			Lateral Bending			Axial Rotation		
		ALL	AB	TTA	ALL	AB	TTA	ALL	AB	TTA
Annulus fibrosis vM stress	R^2	0.723	0.527	0.780	0.536	0.277	0.531	0.545	0.341	0.702
	p	0.000	0.000	0.000	0.000	0.000	0.000	0.000	0.000	0.000
Facet joint contact force	p	0.000	0.000	0.000						
	R^2	0.074	0.107	0.225	0.208	0.686	0.220	0.594	0.282	0.950
	p	0.000*	0.000*	0.000*	0.000	0.000	0.000	0.000	0.000	0.000
Intradiscal pressure	R^2	0.086*	0.164*	0.268*						
	p	0.705	0.460	0.829	0.500	0.337	0.483	0.551	0.459	0.694
	p	0.000	0.000	0.000	0.000	0.000	0.000	0.000	0.000	0.000

*Facet joint contact force without +/-

stiffness calibrated to closely match the stiffness of the soft tissues in the FE model could help to reduce the discrepancy in kinematics.

Participants with TTA had greater average ranges of trunk-pelvis motion compared to able-bodied participants in all DOF except for the transverse plane, which differed by only 1.42 degrees. Throughout the duration of the sit-to-stand motion, participants with TTA were in a more flexed posture than able-bodied participants. Additionally, participants with TTA leaned and rotated towards their right side as opposed to the opposite occurring for able-bodied participants. Three of the four participants with TTA had their left side amputated and this kinematic result implies that people with an amputation favor their intact limb when performing sit-to-stand, which is in agreement with movement strategies for people with LLA during sitting and standing movements [120, 131, 132].

The means of peak annulus fibrosis vM stress, peak facet joint contact force, and average intradiscal pressure were all greater for participants with TTA as compared with able-bodied participants. However, only average intradiscal pressure at the L3-L4 and L4-L5 levels and averaged across levels was significantly different between participant groups (Table 3.1). This may indicate that the peaks of various tissue-level metrics are not different between TTA and able-bodied participants but that the values of these metrics throughout the duration of the motion are greater for participants with TTA. This finding suggests that it may be more beneficial to focus on movement strategies throughout entire cycles of motion as opposed to peak ranges of motion when studying people with TTA.

The regression analyses for annulus fibrosis vM stress vs. flexion/extension, facet joint contact force vs. axial rotation, and intradiscal pressure vs. flexion/extension predicted more than 50% of the variance in each tissue-level metric for all participants (Table 3.2, Figure 3.5). The residuals vs. fits plots for annulus fibrosis vM stress vs. flexion/extension had increased variance for greater values of flexion which indicates a need to use separate regression models for flexion and extension. The smaller R^2 values for all comparisons (Table 3.2) indicated that the selected regressions are not appropriate for the respective metrics. Additionally,

a multiple linear regression may be more suitable for these comparisons due to kinematic coupling of lumbar spine movements [2]. The R^2 values for all but one of the comparisons were greater for participants with TTA as compared to able-bodied participants. This is an interesting finding that could suggest that people with TTA perform sit-to-stand with a more consistent strategy whereas people without TTA do not. Reduced variability among people with TTA may be related to people with TTA favoring their intact limb during movement [133] and could have potential implications for LBP development [68].

The sample size for this study is one of several limitations. With more participants, the differences between participants with and without TTA and the predictive power for the regression analyses may potentially increase. Additionally, calibration of intervertebral joint stiffness in the musculoskeletal model to match the stiffness of the soft tissues in the FE model could help to improve the multiscale kinematic evaluation for flexion/extension (Figure 3.3). One possibility for future work would be to replace the 3-DOF spherical joint at each intervertebral joint in the musculoskeletal model with 6-DOF bushing elements [83, 130] and calibrate the musculoskeletal model's intervertebral joint stiffness to match that of the FE model. Lastly, the geometry for the musculoskeletal and FE models were taken from an average male lumbar spine and scaled in size to each participant. Incorporating subject-specific lumbar spine geometry and lordosis from imaging methods would help to represent each participant's physiology more accurately and may improve the muscle force and joint loading estimates from the musculoskeletal model [134].

3.6 Conclusions

A multiscale model of the lumbar spine was successfully developed to help identify and characterize the interconnectivity between whole-body biomechanics and tissue-level metrics leading to LBP for people with a unilateral transtibial amputation (TTA) during sit-to-stand. Different movement strategies were found between participants with and without TTA which lead to differences in values for various metrics at the tissue-level. Certain motions proved to predict trends in tissue loads well (i.e. flexion/extension and annulus fibrosis vM stress) and

coupled motions may help improve tissue-level metric predictions in future analyses. This research can be extended for use with subject-specific geometries and other populations, such as people with a transfemoral amputation.

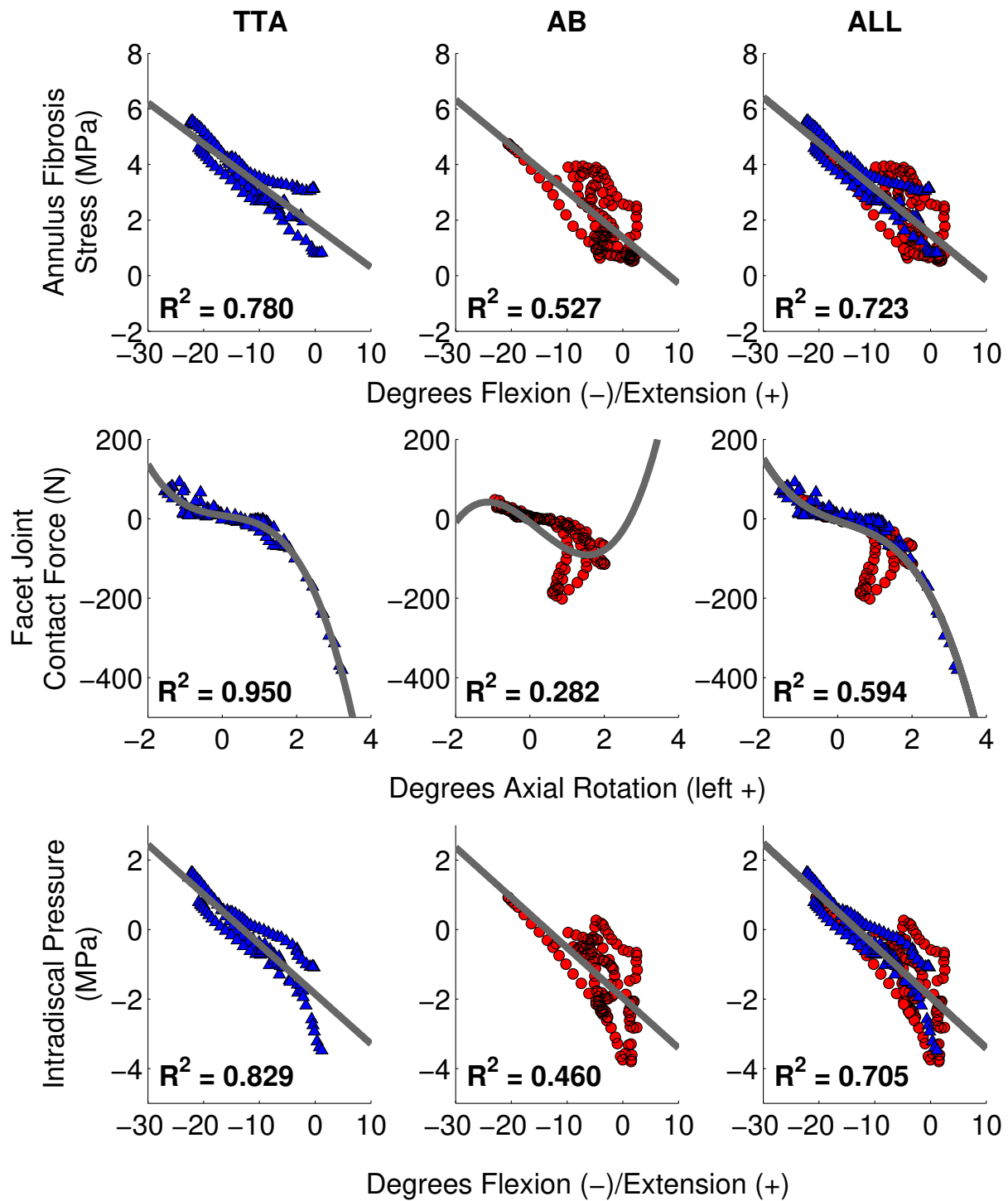


Figure 3.5: Regression model results (grey curves) for annulus fibrosis vM stress vs. flexion/extension, facet joint contact force vs. axial rotation, and intradiscal pressure vs. flexion/extension for each participant group (TTA (blue triangles): participants with TTA, AB (red circles): able-bodied participants, ALL: all participants). R^2 values are indicated for each comparison.

CHAPTER 4

CONCLUSIONS

The purpose of this research was to create a multiscale model of the human lumbar spine to identify and characterize the link between whole-body biomechanics and tissue-level metrics leading to LBP. The model was constructed by combining musculoskeletal and finite element (FE) modeling techniques. Experimental kinematic and kinetic data were collected from people with ($n = 4$) and without ($n = 4$) a unilateral transtibial amputation (TTA) during sit-to-stand and applied to the multiscale model. People with TTA had different movement strategies than able-bodied participants, which led to differences in tissue-level metrics. Regression models for certain motions proved to predict trends in tissue loads quite well, such as flexion/extension vs. annulus fibrosis vM stress and intradiscal pressure. In the future, implementing intervertebral joint stiffness in the musculoskeletal model will be necessary so that the kinematics of the MSM and FE model can converge. Intervertebral joint bushings can be defined in the MSM and the stiffness between the MSM joint bushings and FE intervertebral discs can be calibrated. Additionally, people with a lower-limb amputation, both TTA and TFA, can develop LBP. This study only focuses on people with TTA. A further extension can be to develop a unilateral, TFA musculoskeletal model and apply TFA experimental data to the multiscale model. Finally, due to inter-subject variability, people can have vastly different values for their tissue properties and it could be of interest to quantify the sensitivity of tissue-level metrics to a range of independent parameters such as anatomical shape, ligament and disc properties, and muscle strength. An extension of this work could be to perform a probabilistic analysis with the multiscale model to quantify the sensitivity of metrics that may correlate with LBP such as facet forces, intervertebral disc pressure, and ligament strain.

REFERENCES CITED

- [1] David C Morgenroth, Michael S Orendurff, Ali Shakir, Ava Segal, Jane Shofer, and Joseph M Czerniecki. The relationship between lumbar spine kinematics during gait and low-back pain in transfemoral amputees. *American Journal of Physical Medicine & Rehabilitation*, 89(8):635–643, 2010.
- [2] Nikolai Bogduk. *Clinical and radiological anatomy of the lumbar spine*. Elsevier/Churchill Livingstone, Edinburgh, 5th edition, 2012. ISBN 9780702043420.
- [3] MJ Burke, V Roman, and V Wright. Bone and joint changes in lower limb amputees. *Annals of the Rheumatic Diseases*, 37(3):252–254, 1978.
- [4] Douglas G Smith, Dawn M Ehde, Marcia W Legro, Gayle E Reiber, Michael del Aguila, and David A Boone. Phantom limb, residual limb, and back pain after lower extremity amputations. *Clinical orthopaedics and related research*, 361:29–38, 1999.
- [5] Dawn M Ehde, Douglas G Smith, Joseph M Czerniecki, Kellye M Campbell, Dee M Malchow, and Lawrence R Robinson. Back pain as a secondary disability in persons with lower limb amputations. *Archives of physical medicine and rehabilitation*, 82(6):731–734, 2001.
- [6] Adam J Yoder, Anthony J Petrella, and Anne K Silverman. Trunk–pelvis motion, joint loads, and muscle forces during walking with a transtibial amputation. *Gait & posture*, 41(3):757–762, 2015.
- [7] Blausen.com staff. Blausen gallery - lumbar spine. *Wikiversity Journal of Medicine*, 2014.
- [8] Anatomography. Lumbar vertebra 5. *Licensed under CC BY-SA 2.1 JP*, 7 December 2012.
- [9] Yi Feng, Brian Egan, and Jinxi Wang. Genetic factors in intervertebral disc degeneration. *Genes & Diseases*, 2016.
- [10] National Institute of Neurological Disorders and Stroke (NINDS). Low back pain fact sheet, 2014.
- [11] Harold Ed Merskey. Classification of chronic pain: Descriptions of chronic pain syndromes and definitions of pain terms. *Pain*, 1986.

- [12] F Dudley Hart, D Strickland, and P Cliffe. Measurement of spinal mobility. *Annals of the rheumatic diseases*, 33(2):136, 1974.
- [13] Mark Percy, Ian Portek, and Janis Shepherd. Three-dimensional x-ray analysis of normal movement in the lumbar spine. *Spine*, 9(3):294–297, 1984.
- [14] MJ Percy and SB Tibrewal. Axial rotation and lateral bending in the normal lumbar spine measured by three-dimensional radiography. *Spine*, 9(6):582–587, 1984.
- [15] Robert Roaf. A study of the mechanics of spinal injuries. *Journal of Bone & Joint Surgery, British Volume*, 42(4):810–823, 1960.
- [16] Hickey D Stephen and David WL Hukins. Relation between the structure of the annulus fibrosus and the function and failure of the intervertebral disc. *Spine*, 5(2):106–116, 1980.
- [17] MA Adams and P Dolan. Recent advances in lumbar spinal mechanics and their clinical significance. *Clinical Biomechanics*, 10(1):3–19, 1995.
- [18] Paul Brinckmann, Wolfgang Frobin, Eberhard Hierholzer, and Manfred Horst. Deformation of the vertebral end-plate under axial loading of the spine. *Spine*, 8(8):851–856, 1983.
- [19] Y King Liu, Glen Njus, Joseph Buckwalter, and Koichi Wakano. Fatigue response of lumbar intervertebral joints under axial cyclic loading. *Spine*, 8(8):857–865, 1983.
- [20] TH Hansson, TS Keller, and DM Spengler. Mechanical behavior of the human lumbar spine. ii. fatigue strength during dynamic compressive loading. *Journal of Orthopaedic Research*, 5(4):479–487, 1987.
- [21] James Heilman. L4 vertebra compression fracture post fall from a height. *Wikimedia Commons*, CC BY-SA 3.0 License, 2008.
- [22] MA Adams, WC Hutton, and JRR Stott. The resistance to flexion of the lumbar intervertebral joint. *Spine*, 5(3):245–253, 1980.
- [23] Vijay K Goel, LM Voo, James N Weinstein, Y King Liu, Tetsuo Okuma, and Glen O Njus. Response of the ligamentous lumbar spine to cyclic bending loads. *Spine*, 13(3):294–300, 1988.
- [24] James Heilman. Spondylolisthesis l5/s1. *Wikimedia Commons*, CC BY-SA 4.0 License, 2016.

- [25] Bernard S Epstein. The spine. a radiological text and atlas. *Academic Medicine*, 37(5):526, 1962.
- [26] Nikolai Bogduk, AS Wilson, and Wendy Tynan. The human lumbar dorsal rami. *Journal of anatomy*, 134(Pt 2):383, 1982.
- [27] B Vernon-Roberts and CJ Pirie. Degenerative changes in the intervertebral discs of the lumbar spine and their sequelae. *Rheumatology*, 16(1):13–21, 1977.
- [28] HF Farfan, JW Cossette, GH Robertson, RV Wells, and H Kraus. The effects of torsion on the lumbar intervertebral joints: the role of torsion in the production of disc degeneration. *J Bone Joint Surg Am*, 52(3):468–497, 1970.
- [29] YK Liu, VK Goel, ALF Dejong, G Njus, K Nishiyama, and J Buckwalter. Torsional fatigue of the lumbar intervertebral joints. *Spine*, 10(10):894–900, 1985.
- [30] Ove Svendsen, C Nick Edwards, Brian Lauritzen, and Allan D Rasmussen. Intramuscular injection of hypertonic saline: in vitro and in vivo muscle tissue toxicity and spinal neurone c-fos expression. *Basic & clinical pharmacology & toxicology*, 97(1):52–57, 2005.
- [31] Nikolai Bogduk. Lumbar dorsal ramus syndrome. *The Medical Journal of Australia*, 2(10):537–541, 1980.
- [32] JH Kellgren. Observations on referred pain arising from muscle. *Clin Sci*, 3(176):1937–38, 1938.
- [33] MO Roland. A critical review of the evidence for a pain-spasm-pain cycle in spinal disorders. *Clinical Biomechanics*, 1(2):102–109, 1986.
- [34] William E Garrett, Pantelis K Nikolaou, Beth M Ribbeck, Richard R Glisson, Anthony V Seaber, et al. The effect of muscle architecture on the biomechanical failure properties of skeletal muscle under passive extension. *The American Journal of Sports Medicine*, 16(1):7–12, 1988.
- [35] William E Garrett, Marc R Safran, Anthony V Seaber, Richard R Glisson, Beth M Ribbeck, et al. Biomechanical comparison of stimulated and nonstimulated skeletal muscle pulled to failure. *The American journal of sports medicine*, 15(5):448–454, 1987.
- [36] Pantelis K Nikolaou, Beth L Macdonald, Richard R Glisson, Anthony V Seaber, William E Garrett, et al. Biomechanical and histological evaluation of muscle after controlled strain injury. *The American journal of sports medicine*, 15(1):9–14, 1987.

- [37] DG Simons. Myofascial trigger points: a need for understanding. *Archives of physical medicine and rehabilitation*, 62(3):97–99, 1981.
- [38] DG Simons. Myofascial pain syndromes: where are we? where are we going? *Archives of physical medicine and rehabilitation*, 69(3 Pt 1):207–212, 1988.
- [39] Janet Travell and Seymour H Rinzler. The myofascial genesis of pain. *Postgraduate Medicine*, 11(5):425–434, 1952.
- [40] AE Sola and JH Kuitert. Quadratus lumborum myofasciitis. *Northwest medicine*, 53(10):1003–1005, 1954.
- [41] David Parmenter. Schematic of a trigger point. *Wikimedia Commons*, CC BY-SA 3.0 License, 2014.
- [42] F Kendall, E McCreary, and P Provance. Muscles testing and function (4th edn) williams and wilkins. *Baltimore, Maryland*, 1993.
- [43] Christopher M Norris. Spinal stabilisation: 4. muscle imbalance and the low back. *Physiotherapy*, 81(3):127–138, 1995.
- [44] Dan Carr, Lars Gilbertson, John Frymoyer, Martin Krag, and Malcolm Pope. Lumbar paraspinal compartment syndrome: A case report with physiologic and anatomic studies. *Spine*, 10(9):816–820, 1985.
- [45] David Peck, Paul J Nicholls, Craig Beard, and John R Allen. Are there compartment syndromes in some patients with idiopathic back pain? *Spine*, 11(5):468–475, 1986.
- [46] J Kelgren. On the distribution of pain arising from deep somatic structures with charts of segmental pain area. *Clin Sci*, 4:35–46, 1939.
- [47] Pentti M Rissanen. The surgical anatomy and pathology of the supraspinous and interspinous ligaments of the lumbar spine with special reference to ligament ruptures. *Acta Orthopaedica Scandinavica*, 31(sup46):3–100, 1960.
- [48] Daniel HK Chow, Keith DK Luk, John CY Leong, and CW Woo. Torsional stability of the lumbosacral junction: Significance of the iliolumbar ligament. *Spine*, 14(6):611–615, 1989.
- [49] John CY Leong, Keith DK Luk, Daniel HK Chow, and CW Woo. The biomechanical functions of the iliolumbar ligament in maintaining stability of the lumbosacral junction. *Spine*, 12(7):669–674, 1987.

- [50] I Yamamoto, MM Panjabi, TR Oxland, and JJ Crisco. The role of the iliolumbar ligament in the lumbosacral junction. *Spine*, 15(11):1138–1141, 1990.
- [51] Joseph D Fortin, Anthony P Dwyer, Scott West, and John Pier. Sacroiliac joint: Pain referral maps upon applying a new injection/arthrography technique: Part i: Asymptomatic volunteers. *Spine*, 19(13):1475–1482, 1994.
- [52] Jean-Yves Maigne, Alain Aivaliklis, and Fabrice Pfefer. Results of sacroiliac joint double block and value of sacroiliac pain provocation tests in 54 patients with low back pain. *Spine*, 21(16):1889–1892, 1996.
- [53] Anthony C Schwarzer, Charles N Aprill, and Nikolai Bogduk. The sacroiliac joint in chronic low back pain. *Spine*, 20(1):31–37, 1995.
- [54] Vert Mooney and James Robertson. The facet syndrome. *Clinical Orthopaedics and related research*, 115:149–157, 1976.
- [55] Jeremy CT Fairbank, William M Park, Iain W McCallL, and John P O’Brien. Apophyseal injection of local anesthetic as a diagnostic aid in primary low-back pain syndromes. *Spine*, 6(6):598–605, 1981.
- [56] Anthony C Schwarzer, Charles N Aprill, Richard Derby, Joseph Fortin, Garrett Kine, and Nikolai Bogduk. Clinical features of patients with pain stemming from the lumbar zygapophysial joints: Is the lumbar facet syndrome a clinical entity?. *Spine*, 19(10):1132–1137, 1994.
- [57] AC Schwarzer, CN Aprill, R Derby, J Fortin, G Kine, and N Bogduk. The false-positive rate of uncontrolled diagnostic blocks of the lumbar zygapophysial joints. *Pain*, 58(2):195–200, 1994.
- [58] Anthony C Schwarzer, Shih-chang Wang, Nikolai Bogduk, PJ McNaught, and R Laurent. Prevalence and clinical features of lumbar zygapophysial joint pain: a study in an australian population with chronic low back pain. *Annals of the rheumatic diseases*, 54(2):100–106, 1995.
- [59] King H Yang and AI King. Mechanism of facet load transmission as a hypothesis for low-back pain. *Spine*, 9(6):557–565, 1984.
- [60] N Bogduk and G Jull. The theoretical pathology of acute locked back: a basis for manipulative therapy. *Man Med*, 1(78):67, 1985.

- [61] Barton L Sachs, Heikki Vanharanta, Mark A Spivey, Richard D Guyer, Tapio Videman, Ralph F Rashbaum, Robert G Johnson, Stephen H Hochschuler, and Vert Mooney. Dallas discogram description a new classification of ct/discography in low-back disorders. *Spine*, 12(3):287–294, 1987.
- [62] Donal S McNally, Ian M Shackelford, Allen E Goodship, and Robert C Mulholland. In vivo stress measurement can predict pain on discography. *Spine*, 21(22):2580–2587, 1996.
- [63] Anthony C Schwarzer, Charles N Aprill, Richard Derby, Joseph Fortin, Garrett Kine, and Nikolai Bogduk. The prevalence and clinical features of internal disc disruption in patients with chronic low back pain. *Spine*, 20(17):1878–1883, 1995.
- [64] OpenStax College. Intervertebral disk. *Licensed under CC BY 3.0*, 2013.
- [65] Sandrine Plouvier, Emilie Renahy, Jean-François Chastang, Sébastien Bonenfant, and Annette Leclerc. Biomechanical strains and low back disorders: quantifying the effects of the number of years of exposure on various types of pain. *Occupational and environmental medicine*, 65(4):268–274, 2008.
- [66] Els Clays, Dirk De Bacquer, Françoise Leynen, Marcel Kornitzer, France Kittel, and Guy De Backer. The impact of psychosocial factors on low back pain: longitudinal results from the belstress study. *Spine*, 32(2):262–268, 2007.
- [67] J Kulkarni, WJ Gaine, JG Buckley, JJ Rankine, and J Adams. Chronic low back pain in traumatic lower limb amputees. *Clinical rehabilitation*, 19(1):81–86, 2005.
- [68] Hemakumar Devan, Paul Hendrick, Daniel Cury Ribeiro, Leigh A Hale, and Allan Carman. Asymmetrical movements of the lumbopelvic region: Is this a potential mechanism for low back pain in people with lower limb amputation? *Medical hypotheses*, 82(1):77–85, 2014.
- [69] Hélène Goujon-Pillet, Emilie Sapin, Pascale Fodé, and François Lavaste. Three-dimensional motions of trunk and pelvis during transfemoral amputee gait. *Archives of physical medicine and rehabilitation*, 89(1):87–94, 2008.
- [70] Stephanie B Michaud, Steven A Gard, and Dudley S Childress. A preliminary investigation of pelvic obliquity patterns during gait in persons with transtibial and transfemoral amputation. *Journal of rehabilitation research and development*, 37(1):1, 2000.

- [71] Erik C Prinsen, Marc J Nederhand, and Johan S Rietman. Adaptation strategies of the lower extremities of patients with a transtibial or transfemoral amputation during level walking: a systematic review. *Archives of physical medicine and rehabilitation*, 92(8):1311–1325, 2011.
- [72] Karen Friel, Elizabeth Domholdt, and Douglas G Smith. Physical and functional measures related to low back pain in individuals with lower-limb amputation: an exploratory pilot study. *Journal of rehabilitation research and development*, 42(2):155, 2005.
- [73] Brad D Hendershot and Erik J Wolf. Three-dimensional joint reaction forces and moments at the low back during over-ground walking in persons with unilateral lower-extremity amputation. *Clinical Biomechanics*, 29(3):235–242, 2014.
- [74] Scott L Delp and J Peter Loan. A graphics-based software system to develop and analyze models of musculoskeletal structures. *Computers in biology and medicine*, 25(1):21–34, 1995.
- [75] Michael Damsgaard, John Rasmussen, Søren Tørholm Christensen, Egidijus Surma, and Mark De Zee. Analysis of musculoskeletal systems in the anybody modeling system. *Simulation Modelling Practice and Theory*, 14(8):1100–1111, 2006.
- [76] Scott L Delp, Frank C Anderson, Allison S Arnold, Peter Loan, Ayman Habib, Chand T John, Eran Guendelman, and Darryl G Thelen. Opensim: open-source software to create and analyze dynamic simulations of movement. *Biomedical Engineering, IEEE Transactions on*, 54(11):1940–1950, 2007.
- [77] Felix E Zajac. Muscle coordination of movement: a perspective. *Journal of Biomechanics*, 26:109–124, 1993.
- [78] Scott L Delp, J Peter Loan, Melissa G Hoy, Felix E Zajac, Eric L Topp, and Joseph M Rosen. An interactive graphics-based model of the lower extremity to study orthopaedic surgical procedures. *IEEE Transactions on Biomedical engineering*, 37(8):757–767, 1990.
- [79] Frank C Anderson and Marcus G Pandy. A dynamic optimization solution for vertical jumping in three dimensions. *Computer methods in biomechanics and biomedical engineering*, 2(3):201–231, 1999.
- [80] Frank C Anderson and Marcus G Pandy. Dynamic optimization of human walking. *Journal of biomechanical engineering*, 123(5):381–390, 2001.

- [81] Mark De Zee, Lone Hansen, Christian Wong, John Rasmussen, and Erik B Simonsen. A generic detailed rigid-body lumbar spine model. *Journal of biomechanics*, 40(6):1219–1227, 2007.
- [82] Miguel Christophy, Nur Adila Faruk Senan, Jeffrey C Lotz, and Oliver M OReilly. A musculoskeletal model for the lumbar spine. *Biomechanics and modeling in mechanobiology*, 11(1-2):19–34, 2012.
- [83] Xiangjie Meng, Alexander G Bruno, Bo Cheng, Wenjun Wang, Mary L Bouxsein, and Dennis E Anderson. Incorporating six degree-of-freedom intervertebral joint stiffness in a lumbar spine musculoskeletal model method and performance in flexed postures. *Journal of biomechanical engineering*, 137(10):101008, 2015.
- [84] Kap-Soo Han, Thomas Zander, William R Taylor, and Antonius Rohlmann. An enhanced and validated generic thoraco-lumbar spine model for prediction of muscle forces. *Medical engineering & physics*, 34(6):709–716, 2012.
- [85] Alexander G Bruno, Mary L Bouxsein, and Dennis E Anderson. Development and validation of a musculoskeletal model of the fully articulated thoracolumbar spine and rib cage. *Journal of biomechanical engineering*, 137(8):081003, 2015.
- [86] Dominika Ignasiak, Sebastian Dendorfer, and Stephen J Ferguson. Thoracolumbar spine model with articulated ribcage for the prediction of dynamic spinal loading. *Journal of biomechanics*, 49(6):959–966, 2016.
- [87] Michael Putzer, Ingo Ehrlich, John Rasmussen, Norbert Gebbeken, and Sebastian Dendorfer. Sensitivity of lumbar spine loading to anatomical parameters. *Journal of biomechanics*, 49(6):953–958, 2016.
- [88] Thomas Zander, Marcel Dreischarf, Hendrik Schmidt, Georg Bergmann, and Antonius Rohlmann. Spinal loads as influenced by external loads: A combined in vivo and in silico investigation. *Journal of biomechanics*, 48(4):578–584, 2015.
- [89] A Shirazi-Adl. Finite-element evaluation of contact loads on facets of an l2-l3 lumbar segment in complex loads. *Spine*, 16(5):533–541, 1991.
- [90] Francois Lavaste, Wafa Skalli, Stéphane Robin, Raymond Roy-Camille, and Christian Mazel. Three-dimensional geometrical and mechanical modelling of the lumbar spine. *Journal of biomechanics*, 25(10):1153–1164, 1992.
- [91] Vijay K Goel, Weizeng Kong, Jung S Han, James N Weinstein, and Lars G Gilbertson. A combined finite element and optimization investigation of lumbar spine mechanics with and without muscles. *Spine*, 18(11):1531–1541, 1993.

- [92] Marta Kurutz. *Finite element modelling of human lumbar spine*. INTECH Open Access Publisher, 2010.
- [93] Augustus A White, Manohar M Panjabi, et al. *Clinical biomechanics of the spine*, volume 2. Lippincott Philadelphia, 1990.
- [94] Julius Quinn Campbell and Anthony J Petrella. An automated method for landmark identification and finite-element modeling of the lumbar spine. *IEEE Transactions on Biomedical Engineering*, 62(11):2709–2716, 2015.
- [95] Nadine Michele Lalonde, Yvan Petit, Carl-Eric Aubin, Eric Wagnac, and Pierre-Jean Arnoux. Method to geometrically personalize a detailed finite-element model of the spine. *IEEE Transactions on Biomedical Engineering*, 60(7):2014–2021, 2013.
- [96] Frank Niemeyer, Hans-Joachim Wilke, and Hendrik Schmidt. Geometry strongly influences the response of numerical models of the lumbar spine: a probabilistic finite element analysis. *Journal of biomechanics*, 45(8):1414–1423, 2012.
- [97] Won Man Park, Kyungsoo Kim, and Yoon Hyuk Kim. Effects of degenerated intervertebral discs on intersegmental rotations, intradiscal pressures, and facet joint forces of the whole lumbar spine. *Computers in biology and medicine*, 43(9):1234–1240, 2013.
- [98] Antonius Rohlmann, Thomas Zander, Hendrik Schmidt, Hans-Joachim Wilke, and Georg Bergmann. Analysis of the influence of disc degeneration on the mechanical behaviour of a lumbar motion segment using the finite element method. *Journal of biomechanics*, 39(13):2484–2490, 2006.
- [99] Marcel Dreischarf, Aboufazel Shirazi-Adl, Navid Arjmand, Antonius Rohlmann, and Hendrik Schmidt. Estimation of loads on human lumbar spine: a review of in vivo and computational model studies. *Journal of biomechanics*, 49(6):833–845, 2016.
- [100] Hendrik Schmidt, Aboufazel Shirazi-Adl, Fabio Galbusera, and Hans-Joachim Wilke. Response analysis of the lumbar spine during regular daily activities: a finite element analysis. *Journal of biomechanics*, 43(10):1849–1856, 2010.
- [101] Antonius Rohlmann, Lars Bauer, Thomas Zander, Georg Bergmann, and Hans-Joachim Wilke. Determination of trunk muscle forces for flexion and extension by using a validated finite element model of the lumbar spine and measured in vivo data. *Journal of Biomechanics*, 39(6):981–989, 2006.
- [102] Hendrik Schmidt, Maxim Bashkuev, Marcel Dreischarf, Antonius Rohlmann, Georg Duda, Hans-Joachim Wilke, and Aboufazel Shirazi-Adl. Computational biomechanics of a lumbar motion segment in pure and combined shear loads. *Journal of biomechanics*, 46(14):2513–2521, 2013.

- [103] Marcel Dreischarf, Antonius Rohlmann, Rui Zhu, Hendrik Schmidt, and Thomas Zander. Is it possible to estimate the compressive force in the lumbar spine from intradiscal pressure measurements? a finite element evaluation. *Medical engineering & physics*, 35(9):1385–1390, 2013.
- [104] Thomas Zander, Antonius Rohlmann, and Georg Bergmann. Influence of ligament stiffness on the mechanical behavior of a functional spinal unit. *Journal of biomechanics*, 37(7):1107–1111, 2004.
- [105] Hendrik Schmidt, Frank Heuer, Ulrich Simon, Annette Kettler, Antonius Rohlmann, Lutz Claes, and Hans-Joachim Wilke. Application of a new calibration method for a three-dimensional finite element model of a human lumbar annulus fibrosus. *Clinical Biomechanics*, 21(4):337–344, 2006.
- [106] Hendrik Schmidt, Fabio Galbusera, Antonius Rohlmann, and Aboulfazl Shirazi-Adl. What have we learned from finite element model studies of lumbar intervertebral discs in the past four decades? *Journal of biomechanics*, 46(14):2342–2355, 2013.
- [107] M Dreischarf, T Zander, A Shirazi-Adl, CM Puttlitz, CJ Adam, CS Chen, VK Goel, A Kiapour, YH Kim, KM Labus, et al. Comparison of eight published static finite element models of the intact lumbar spine: predictive power of models improves when combined together. *Journal of biomechanics*, 47(8):1757–1766, 2014.
- [108] Merryn Tawhai, Jeff Bischoff, Daniel Einstein, Ahmet Erdemir, Trent Guess, and Jeff Reinbolt. Multiscale modeling in computational biomechanics. *IEEE Engineering in Medicine and Biology Magazine*, 28(3):41–49, 2009.
- [109] Gerard A Ateshian and Morton H Friedman. Integrative biomechanics: A paradigm for clinical applications of fundamental mechanics. *Journal of biomechanics*, 42(10):1444–1451, 2009.
- [110] Steve A Maas, Benjamin J Ellis, Gerard A Ateshian, and Jeffrey A Weiss. Febio: finite elements for biomechanics. *Journal of biomechanical engineering*, 134(1):011005, 2012.
- [111] Susan M Sunkin, Lydia Ng, Chris Lau, Tim Dolbeare, Terri L Gilbert, Carol L Thompson, Michael Hawrylycz, and Chinh Dang. Allen brain atlas: an integrated spatio-temporal portal for exploring the central nervous system. *Nucleic acids research*, 41(D1):D996–D1008, 2013.
- [112] JP Halloran, S Sibole, CC Van Donkelaar, MC Van Turnhout, CWJ Oomens, Jeffrey A Weiss, Farshid Guilak, and Ahmet Erdemir. Multiscale mechanics of articular cartilage: potentials and challenges of coupling musculoskeletal, joint, and microscale computational models. *Annals of biomedical engineering*, 40(11):2456–2474, 2012.

- [113] Richard J van Arkel, Luca Modenese, Andrew Phillips, and Jonathan RT Jeffers. Hip abduction can prevent posterior edge loading of hip replacements. *Journal of Orthopaedic Research*, 31(8):1172–1179, 2013.
- [114] Andrew TM Phillips, Claire C Villette, and Luca Modenese. Femoral bone mesoscale structural architecture prediction using musculoskeletal and finite element modelling. *International Biomechanics*, 2(1):43–61, 2015.
- [115] K McDonald, J Little, M Pearcy, and C Adam. Development of a multi-scale finite element model of the osteoporotic lumbar vertebral body for the investigation of apparent level vertebra mechanics and micro-level trabecular mechanics. *Medical engineering & physics*, 32(6):653–661, 2010.
- [116] Rui Zhu, Thomas Zander, Marcel Dreischarf, Georg N Duda, Antonius Rohlmann, and Hendrik Schmidt. Considerations when loading spinal finite element models with predicted muscle forces from inverse static analyses. *Journal of biomechanics*, 46(7):1376–1378, 2013.
- [117] Stephen R Lord, Susan M Murray, Kirsten Chapman, Bridget Munro, and Anne Tiedemann. Sit-to-stand performance depends on sensation, speed, balance, and psychological status in addition to strength in older people. *The Journals of Gerontology Series A: Biological Sciences and Medical Sciences*, 57(8):M539–M543, 2002.
- [118] Gary LK Shum, Jack Crosbie, and Raymond YW Lee. Three-dimensional kinetics of the lumbar spine and hips in low back pain patients during sit-to-stand and stand-to-sit. *Spine*, 32(7):E211–E219, 2007.
- [119] Guillaume Christe, Lucy Redhead, Thomas Legrand, Brigitte M Jolles, and Julien Favre. Multi-segment analysis of spinal kinematics during sit-to-stand in patients with chronic low back pain. *Journal of biomechanics*, 49(10):2060–2067, 2016.
- [120] Brad D Hendershot and Erik J Wolf. Persons with unilateral transfemoral amputation have altered lumbosacral kinetics during sitting and standing movements. *Gait & posture*, 42(2):204–209, 2015.
- [121] Gary T Yamaguchi and Felix E Zajac. A planar model of the knee joint to characterize the knee extensor mechanism. *Journal of biomechanics*, 22(1):1–10, 1989.
- [122] Michael Reid Carhart. Biomechanical analysis of compensatory stepping: Implications for paraplegics standing via fns. 2001.
- [123] David A Winter. *Biomechanics and motor control of human movement*. John Wiley & Sons, 2009.

- [124] Felix E Zajac. Muscle and tendon properties models scaling and application to biomechanics and motor. *Critical reviews in biomedical engineering*, 17(4):359–411, 1989.
- [125] AK Silverman and RR Neptune. Differences in whole-body angular momentum between below-knee amputees and non-amputees across walking speeds. *Journal of biomechanics*, 44(3):379–385, 2011.
- [126] JA Actis, JD Honegger, DH Gates, AJ Petrella, LA Nolasco, and AK Silverman. Validation of lumbar spine loading from a musculoskeletal model including the lower limbs and lumbar spine. *Submitted to: Journal of biomechanics*, 2017.
- [127] JQ Campbell, DJ Coombs, M Rao, PJ Rullkoetter, and AJ Petrella. Automated finite element meshing of the lumbar spine: Verification and validation with 18 specimen-specific models. *Journal of biomechanics*, 49(13):2669–2676, 2016.
- [128] Jeremy CT Fairbank and Paul B Pynsent. The oswestry disability index. *Spine*, 25(22):2940–2953, 2000.
- [129] T-W Lu and JJ Oconnor. Bone position estimation from skin marker co-ordinates using global optimisation with joint constraints. *Journal of biomechanics*, 32(2):129–134, 1999.
- [130] Miguel Christophy, Maurice Curtin, Nur Adila Faruk Senan, Jeffrey C Lotz, and Oliver M OReilly. On the modeling of the intervertebral joint in multibody models for the spine. *Multibody System Dynamics*, 30(4):413–432, 2013.
- [131] Sebastjan Šlajpah, Roman Kamnik, Helena Burger, Tadej Bajd, and Marko Munih. Asymmetry in sit-to-stand movement in patients following transtibial amputation and healthy individuals. *International Journal of Rehabilitation Research*, 36(3):275–283, 2013.
- [132] Helena Burger, Jernej Kuželčki, and Črt Marinček. Transition from sitting to standing after trans-femoral amputation. *Prosthetics and orthotics international*, 29(2):139–151, 2005.
- [133] Yoshimasa Sagawa, Katia Turcot, Stephane Armand, Andre Thevenon, Nicolas Vuillerme, and Eric Watelain. Biomechanics and physiological parameters during gait in lower-limb amputees: a systematic review. *Gait & posture*, 33(4):511–526, 2011.
- [134] Alexander G Bruno, Hossein Mokhtarzadeh, Brett T Allaire, Kelsey R Velie, M De Paolis Kaluza, Dennis E Anderson, and Mary L Boussein. Incorporation of ct-based measurements of trunk anatomy into subject-specific musculoskeletal models of the spine influences vertebral loading predictions. *Journal of Orthopaedic Research*, 2017.

APPENDIX
SUPPORTING TABLES

Table A.1: The extent to which proposed causes of back pain satisfy the postulates for a structure to be a source of LBP [2]

Structure or cause	Postulates					
	Innervated	Pain in normal volunteers	Pathology known	Identified in patients	Prevalence	
					<i>Acute back pain</i>	<i>Chronic back pain</i>
Vertebral bodies	Yes	No	Yes	Yes	Rare	Rare
Kissing spines	Yes	No	Presumed	Yes	Unknown	Unknown
Lamina impaction	Yes	No	Presumed	No	Unknown	Unknown
Spondylolysis	Yes	No	Yes	Yes	< 6%	< 6%
Muscle sprain	Yes	Yes	Yes	Anecdotal	Unknown	Unknown
Muscle spasm	Yes	Yes	No	No	Unknown	Unknown
Muscle imbalance	Yes	No	No	Uncontrolled	Unknown	Unknown
Trigger points	Yes	Yes	No	Unreliable	Unknown	Unknown
Iliac crest syndrome	Yes	Yes	No	Yes	Unknown	30-50%
Compartment syndrome	Yes	No	No	Yes	Unknown	Unknown
Fat herniation	Yes	No	Yes	Yes	Unknown	Unknown
Dural pain	Yes	Yes	Presumed	Yes	Unknown	Unknown
Epidural plexus	Yes	No	No	No	Unknown	Unknown
Interspinous ligament	Yes	Yes	Presumed	Uncontrolled	Unknown	< 10%
Iliolumbar ligament	Probably	No	No	No	Unknown	Unknown
Sacroiliac joint pain	Yes	Yes	No	Controlled studies	Unknown	13% ($\pm 7\%$)
Zygapophysial joint pain	Yes	Yes	No	Controlled studies	Unknown	< 10%, 32% (elderly)
Internal disc disruption	Yes	No	Yes	Controlled studies	Unknown	39% ($\pm 10\%$)